THE LANCET
Respiratory Medicine

Supplementary appendix 1

This appendix formed part of the original submission and has been peer reviewed. We post it as supplied by the authors.

Supplement to: Feys S, Gonçalves SM, Khan M, et al. Lung epithelial and myeloid innate immunity in influenza-associated or COVID-19-associated pulmonary aspergillosis: an observational study. *Lancet Respir Med* 2022; published online Aug 24. https://doi.org/10.1016/S2213-2600(22)00259-4.

Supplementary Material

Lung epithelial and myeloid immunity in influenza- and COVID-19-associated pulmonary aspergillosis

Simon Feys, Samuel M. Gonçalves*, Mona Khan*, Sumin Choi*, Bram Boeckx, Denis Chatelain, Cristina Cunha, Yves Debaveye, Greet Hermans, Marjan Hertoghs, Stephanie Humblet-Baron, Cato Jacobs, Katrien Lagrou, Lukas Marcelis, Julien Maizel, Philippe Meersseman, Rémy Nyga, Laura Seldeslachts, Marick Rodrigues Starick, Karin Thevissen, Christophe Vandenbriele, Lore Vanderbeke, Greetje Vande Velde, Niels Van Regenmortel, Arno Vanstapel, Sam Vanmassenhove, Alexander Wilmer, Frank L. Van De Veerdonk, Gert De Hertogh, Peter Mombaerts, Diether Lambrechts, Agostinho Carvalho†, Johan Van Weyenbergh†, Joost Wauters†

* Contributed equally

† Shared last authors

Table of contents

Supplementary Methods

Study participants

The study protocol was approved and the need for informed consent waived by the Ethical Committee (EC) of the University Hospitals Leuven, Belgium (S65588). We retrospectively identified all patients who had been admitted to the ICU of the University Hospitals Leuven due to respiratory distress caused by influenza or COVID-19 in the period between 01-01-2011 and 31-03-2021, and of whom BAL samples were available at the hospital biobank. Respiratory distress was defined as a respiratory rate of >= 25x/minute and a P_AO_2/F_IO_2-ratio of < 300 with or without bilateral infiltrates. Diagnosis of influenza or COVID-19 had to be proven by PCR-detection of influenza virus or SARS-CoV-2 on a respiratory sample in the 14 days prior to ICU-admission, or during the first 10 days of ICU admission. The respiratory distress had to be caused primarily by the influenza virus or SARS-CoV-2 infection according to the treating physician. Only patients who had received sufficient work-up for aspergillosis (consisting of chest imaging and bronchoscopy with BAL-fluid sampling for fungal culture and GM testing) were included. Patients with a history of invasive pulmonary aspergillosis prior to hospital admission were excluded. Demographic, clinical, treatment and outcome data was derived from the patient electronic medical records. Diagnosis of probable or proven influenza-associated pulmonary aspergillosis (IAPA) was made based on the consensus criteria as published by Verweij et al.[1] Diagnosis of probable or proven COVID-19-associated pulmonary aspergillosis (CAPA) was based on the ECMM/ISHAM criteria by Koehler et al[2] (since we did not use non-bronchoscopic lavage in our center, we did not retain “possible CAPA” as an option). If a diagnosis of IAPA or CAPA was made in an influenza or COVID-19 patient >14 days after study BAL sample with negative BAL sampling in between, this patient was classified as a non-aspergillosis patient. Using the same criteria, *in vivo* tracheobronchial biopsy samples were collected from IAPA and CAPA patients admitted to the ICU of University Hospitals Leuven (S65588, need for informed consent waived by the Ethical Committee of the University Hospitals Leuven) and Hospital Network Antwerp (Belgium, The Commissie voor Medische Ethiek ZNA; Institutional Review Board – ZNA/OCMW Antwerpen (OG 031-009)

Approval N° 5530, waiver of informed consent obtained to collect pseudonymized data and stored samples obtained as part of standard of care during the first COVID-19 pandemic waves) and Amiens-Picardie University Hospital (France, approval of the Institutional Review Board for Human Subjects, PI2019_843_0047 Nord-Ouest II – France, patients/relatives provided their informed consent).

BAL collection

All BAL samples had been obtained by bronchoscopy as part of clinical routine. BAL sampling was performed by instillation of approximately 20 mL 0·9% sterile saline solution after wedging the bronchus of the right middle lobe if equally affected lobes on imaging, or the most affected lobe on imaging, after which as much fluid as possible was suctioned. Samples were immediately sent to the clinical laboratory, where a small aliquot was used for clinical testing including culture and GM assay. The remainder was immediately stored at the hospital biobank at -20°C until use for this study. For IAPA and CAPA patients, BAL samples showing first mycological evidence of aspergillosis (by culture or positive GM ≥1·0) were selected. In case this sample was not available, the first available sample that still showed arguments for aspergillosis (within maximum five days after initial positive sample) was selected from the biobank. For COVID-19 and influenza patients without aspergillosis, the first sample obtained during ICU admission was selected.

Galactomannan assay

To detect GM presence on uncentrifuged BAL samples, the Platelia *Aspergillus* enzyme immunoassay (EIA) (Bio-Rad, Marnes-la-Coquette, France) was used as part of routine microbiological workup, as previously described.[3] The EIA data was expressed as GM index.

RNA-extraction and nCounter® analysis

RNA was extracted from frozen BAL samples using the RNeasy kit (Qiagen), according to the manufacturer's instructions. Hybridization (65°C for 24 hr) to a Myeloid Innate Immunity panel (V2) of 770 unique nCounter (Nanostring) reporter and capture probes (730 immune genes and 40 housekeeping genes) and Plus Panel (with 25 human immune-related genes used for analysis) was followed by processing on nCounter MAX Prep station and quantification on MAX Digital Analyzer (Nanostring), as previously validated for quantification of host immune transcripts, even with low RNA yield.[4–6]

BAL gene expression analyses

Data was analyzed using ROSALIND® (https://rosalind.onramp.bio/), with a HyperScale architecture developed by ROSALIND, Inc. (San Diego, CA). Read Distribution percentages, violin plots, identity heat maps, and sample MDS plots were generated as part of the QC step. Normalization, fold changes and p-values were calculated using criteria provided by Nanostring. ROSALIND® follows the nCounter Advanced Analysis protocol of dividing counts within a lane by the geometric mean of the normalizer probes from the same lane. Housekeeping probes used for normalization were selected based on the geNorm algorithm as implemented in the NormqPCR R library.[7] Fold changes and p-values (with or without correction for covariates) were calculated using the fast method as described in the nCounter Advanced Analysis 2.0 User Manual (MAN-10030-03). P-value adjustment was performed using the Benjamini-Hochberg (BH) method of estimating false discovery rates (FDR) in ROSALIND® and expressed as q-values. Volcano plots were constructed using the EnhancedVolcano R package[8] as extension to ggplot2[9]. Heat maps of differentially expressed genes ranked to fold change were constructed in Graphpad using ROSALIND®-generated mean subtracted normalized log2 expression values.

BAL CIBERSORTx

CIBERSORTx[10] was used to infer the epithelial and immune cell composition of the BAL samples. For this purpose, we constructed a novel signature matrix as there is currently no signature matrix available for BAL-fluid specifically. We used a scRNA-seq expression matrix of the marker genes of BAL-fluid cell subtypes (without mast cells and dendritic cells, as their counts were extremely low) derived from the critically ill patients in the study of Wauters et al[11] as input file. We found an overlap of 226 genes between the genes in our nCounter-panel and the genes in the expression matrix input file. For each gene, z-scores among all cell subtypes were calculated. For each cell subtype, the five genes with the highest z-score were selected to be implemented in the signature matrix. Duplicate genes were removed. Normalized gene counts as found in the expression

matrix were implemented in the signature matrix, which eventually consisted of 143 genes. Normalized gene counts from our BAL samples were processed in CIBERSORTx (relative mode) with 1000 permutations. The cell subtypes obtained were summarized into 8 major cell types. Only samples with p-value <0·05 (demonstrating statistical significance of the results obtained by deconvolution across the cell subsets) were included. Correlograms using Spearman's correlation were plotted.

BAL ClueGO and GSEA pathway analyses

The ClueGO plug-in was used in Cytoscape to perform pathway analysis using a hypergeometric enrichment test[12]. All negative differentially expressed genes (DEGs) from IAPA vs. influenza-only, CAPA vs. COVID-19-only, influenza-only vs. COVID-19-only and IAPA vs. CAPA (the three first groups DEG with q-value <0·05, the latter with q-value <0·20 as too few DEGs with q-value <0·20 were present to allow this kind of pathway analysis) were used as input genes and GO Biological Processes as ontology library, with selection of pathways with minimum 3 genes or 2% of pathway genes overlap with the input DEG list, and with fusion of multiple GO levels as performed by ClueGO. Correction for multiple testing was performed using Benjamini-Hochberg (BH). Dot plot construction was performed in R using ggplot2.[9] Terms overlapping between groups were included, and for each group separately the remaining non-redundant terms were selected for incorporation in a dot plot, eventually showing the 18 terms with the largest gene counts. Chord plots were constructed for all disease comparisons.

Gene Set Enrichment Analysis (GSEA) was performed with GSEA 4.2.3[13] on the normalized expression data generated by Rosalind®, using 1000 permutations. Reactome canonical pathways were selected from the Molecular Signatures Database (MSigDB, version 7.5).[14] We accessed the enrichment scores for pathways with minimum 15 and maximum 500 genes shared with our data, and minimum 15% pathway coverage. BH method was used to correct for multiple testing. The number of genesets tested was 51. Enrichment and leading-edge subset plots were generated for all tested pathways and are shown for the depicted pathways.

BAL pathway module scores

Pathway module scores were calculated for the IL-1β, TNF-α, type I IFN, type II IFN pathways using the validated module by Bell et al[15] (IL-1β) and the gene lists of Waddell et al[16] (TNF-α, type I & II IFN) as input. For each signature, the overlapping genes between the input file and the nCounter panel were selected for further analysis. Z-scores were calculated for each gene among all four disease groups using log2 normalized gene counts, and the median Z-score of each gene per disease group was plotted in a heat map for each gene module. Per patient, a gene module score was calculated for the aforementioned pathways using the geometric mean of the normalized gene counts, and these gene module scores were plotted in violin plots.

BAL protein analyses

The protein levels of cytokines, chemokines, and other inflammatory mediators in BAL samples were measured using the 44-plex Human XL Cytokine Fixed Panel (R&D Systems), the 13-plex LEGENDplex Human Anti-Virus Response Panel (BioLegend), and ELISA MAX Deluxe Set kits for IL-8 and PTX3 (BioLegend), according to the manufacturer's instructions. For viral inactivation, samples (and standards) were treated before analyses for 30 min with 10% formalin, followed by washing and resuspension in the appropriate buffer. Depending on the assay, analyses were performed using a Bio-Plex MAGPIX Multiplex Reader, a BD LSR II flow cytometer or a Tecan Infinite 200 PRO plate reader, respectively. All cytokine determinations were performed in duplicates. For cytokines overlapping in the multiplex panels, the 44-plex kit results were used for further analyses, while for IL-8 the ELISA MAX Deluxe Set kit result was used. Outliers were identified and removed using Grubb's test (alpha 0·05). Missing data were left out of the analyses. Protein levels are expressed in pg/mL.

Histopathology and RNAscope analyses of tracheobronchial biopsy samples

FFPE tracheobronchial biopsy samples, obtained *in vivo* as part of clinical routine during ICU-stay because of visualization of ulceration on bronchoscopy, were sectioned at 5µm and collected on SuperFrost Plus Gold slides (Thermo Fisher Scientific/Menzel Gläser, Cat#K5800AMNZ72). For each biopsy sample, four neighboring sections were stained with H&E, used for spatial transcriptomics, used for RNAscope and stained with Grocott-

Gomori's methenamine silver (GMS) staining respectively. One IAPA biopsy sample consisted of two separate parts, taken at the same timepoint. After collection, slides intended for spatial transcriptomics and RNAscope were air-dried at room temperature, after which slides were stored in dry conditions at 4°C until further use. Slides intended for H&E and GMS staining were heated overnight at 56°C prior to staining. H&E stainings were performed using a fully automated H&E platform (Dako CoverStainer, Agilent). GMS stainings were performed using the Artisan Link Pro Special Staining System. Images of H&E and GMS stainings were taken with a Phillips IntelliSite Ultra Fast Scanner.

We used the fluorescence RNAscope platform to visualize influenza virus and SARS-CoV-2 RNA in the tracheobronchial sections. RNAscope manual assay was performed using the Multiplex Fluorescent Detection Kit v2 (Advanced Cell Diagnostics, Cat#323110) according to manufacturer's protocols. Briefly, slides were baked at 60°C for 1 hr, then deparaffinized in Xylene (Leica Biosystems, Cat#3803665EG). Slides were pretreated with hydrogen peroxide at room temperature for 15 min, followed by permeabilization in target retrieval reagent (Advanced Cell Diagnostics, Cat#322000) for 15 min in a steamer, and digestion with Protease Plus (Advanced Cell Diagnostics, Cat#322330) at 40°C for 20 min. RNAscope probe V-nCoV-N-C1 (Advanced Cell Diagnostics, Cat #846081) was hybridized at 40°C for 2 hr. Signal amplification was followed by development of HRP channel with dye Opal 520 (Akoya Biosciences, Cat#FP1487001KT) at 1:1500 in 1x Plus Amplification Diluents (Akoya Biosciences, Cat#FP1498). Immunohistochemistry was performed after the final step of HRP blocker application. Slides were blocked in 10% donkey serum (Sigma-Aldrich, Cat#S30-100ML) in 0.1% Triton/PBS at room temperature for 1 hr. Mouse monoclonal anti-human Cytokeratin 8, KRT8 antibody (R&D Systems, Cat#MAB3165) was used at 1:200 in 2% donkey serum in 0.1% Triton/PBS and incubated at 4°C overnight. Slides were then washed in 0·1% Triton/PBS 3 x 5 min each followed by incubation with Alexa Fluor Plus 555 donkey anti-rabbit (Thermo Fisher Scientific, Cat#A32794) at 1:500 in 2% normal donkey serum in 0.1% Triton/PBS at room temperature for 1 hr. DAPI (Thermo Fisher Scientific, Cat#D1306) served as nuclear stain. Slides were mounted in Mount Solid antifade (abberior, Cat#MM-2011-2X15ML). Confocal images were taken with the Zeiss ZEN 2.6 system on a Zeiss LSM 800.

Spatial transcriptomics using GeoMx®

In brief, we evaluated the sections of the IAPA and CAPA IATB biopsies with the GeoMx® Digital Spatial Profiler (DSP) using the Whole Transcriptome Atlas catalog with a SARS-CoV-2 spike-in, which completely covers the range of protein coding genes as well as a selection of SARS-CoV-2 genes.[17] In total, six epithelial regions of interest (ROIs) and five subepithelial ROIs with inflammatory infiltrate were selected in the IAPA biopsies, while three epithelial ROIs and three subepithelial ROIs with inflammatory infiltrate were selected in the CAPA biopsies.

We followed the GeoMx DSP user manuals for GeoMx DSP slide preparation (MAN-10115-05), GeoMx DSP sample collection (SEV-00087-05), GeoMx DSP library preparation (MAN-10117-05) and GeoMx DSP data analysis (SEV-00090-05). In brief, tissue slides were baked at 60°C for 1h in a drying oven after which they were deparaffinized and rehydrated using a Leica Biosystems FFPE BOND RX. RNA targets were exposed using proteinase K solution followed by fixation using 10% NBF. After unloading the tissue slides from the Leica Biosystems BOND RX, they were incubated overnight with the RNA probe mix (Whole Transcriptome Atlas, which consists of in situ hybridization probes with UV photocleavable oligonucleotide barcodes). Tissues were then washed and stained with the visualization markers: panCK-488 at 1:600 (Invitrogen, NBP2-33200AF488), CD45-594 at 1:100 (CST, 13917BF), CD68-647 at 1:400 (Santa Cruz, sc-20060AF647) and SYTO 83 at 1:25 (Fisher, S11364).

Tissue slides were then loaded in and scanned with the GeoMx DSP instrument. In conjunction with a pathologist, we selected epithelial ROIs and subepithelial inflammatory infiltrate ROIs using the immunohistochemistry markers on the slide and the H&E and GMS stainings of the neighboring slides as guide. Serial UV illumination of each ROI was used to collect the probe barcodes from the different ROIs. Using the i5/i7 dual-indexing system of Illumina, each ROI was uniquely indexed. An Illumina NovaSeq was used for pair-end sequencing (2 x 75) of libraries, after which the obtained data was processed and filtered for quality. FASTQ files for each ROI were demultiplexed and converted to digital count conversion (DCC) files using the GeoMx NGS Pipeline (version 2.3.4) application. The DCCs were transferred to the GeoMx DSP Data Analysis

Suite, which was used to align ROIs with raw and Q3 (3rd quartile of all selected targets) normalized counts of all targets. Q3 normalization uses the top 25% of expressors to normalize across ROIs, which makes this strategy robust to changes in expression of individual genes and suited for making comparisons across ROIs. Differential expression between IAPA and CAPA epithelial ROIs and inflammatory infiltrate ROIs was investigated using a linear mixed model accounting for patient ID and presence of viral positivity on RNAscope in the ROI and t-test respectively, and DEGs were plotted using EnhancedVolcano.[8] To assess concordant differences between IAPA and CAPA, gene set enrichment analysis (GSEA)[13] was performed on the Q3 normalized data of the epithelial ROIs with GSEA 4.2.3[13] with 1000 permutations. Reactome canonical pathways were selected from the Molecular Signatures Database (MSigDB, version 7.5).[14] We accessed the enrichment scores for pathways with minimum 25 and maximum 500 genes shared with our data, and minimum 15% pathway coverage. Using these criteria, 744 gene sets were used for analysis. A subset of terms for the epithelial comparison was plotted. Correction for multiple testing was performed using BH method. Enrichment and leading-edge subset plots were generated for all pathways and are shown for the depicted pathways.

Statistical analyses

Unless stated otherwise in the (supplementary) methods, statistical testing was performed with correction for multiple testing Kruskal-Wallis test with follow-up Benjamini-Krieger-Yekutieli (BKY) two-stage step-up method for CIBERSORTx cell fractions, pathway module scores and protein levels. The more conservative Benjamini-Hochberg (BH) method was used for correction for multiple testing in the nCounter and GeoMx gene expression analyses. Adjusted p-values are reported as q-values. A two-sided alternative hypothesis at the 5% significance level was used for statistical analyses, except for GSEA for which the recommended 25% significance level was used.[13] Correlation analyses were performed and plotted using Spearman's correlation using the R packages ggpubr[18] and corrplot[19] in R version 4.1.0.-Unless stated otherwise in the (supplementary) methods, the other statistical analyses were performed using GraphPad Prism 9.2.0 for Windows, GraphPad Software, San Diego, California USA, www.graphpad.com.

Supplementary Tables

Supplementary Table 1. Clinical characteristics of included patients with nCounter analyses (n=134).

	Influenza-only (n = 35)	IAPA (n = 38)	COVID-19-only (n = 34)	CAPA (n = 27)
Mean age – years (SD)	61 (2·3)	61 (2·3)	62 (11)	71 (9)
Male sex	18 (51%)	25 (66%)	26 (76%)	24 (89%)
Median BMI (IQR)	26 (10)	26 (7·9)	31 (10)	28 (9·9)
Diabetes mellitus	9 (26%)	6 (16%)	15 (44%)	10 (37%)
Liver cirrhosis	0	0	0	0
COPD	6 (17%)	10 (26%)	3 (9%)	5 (19%)
EORTC/MSGERC host factor*	10 (29%)	14 (37%)	0	3 (11%)
Hematologic malignancy	1 (3%)	4 (11%)	0	0
Allogeneic HSCT	1 (3%)	2 (5%)	0	0
Solid organ transplant	4 (11%)	8 (21%)	0	1 (4%)
Neutropenia	0	3 (8%)	0	0
Prolonged high-dose CS	3 (9%)	2 (5%)	0	0
Immunosuppressants	6 (17%)	11 (29%)	0	3 (11%)
Cytotoxic agents	2 (6%)	3 (8%)	0	1 (4%)
Median Charlson Comorbidity Index at ICU admission (IQR)	4 (5)	3 (4)	3 (2)	5 (1)
Median APACHE II score at ICU admission (IQR)	27 (9) n = 34	28 (16) n = 36	26 (16) n = 26	23 (10) n = 23
Received MV	33 (94%)	32 (84%)	34 (100%)	27 (100%)
Median days of MV (IQR)	10 (15)	12 (21)	21 (21)	15 (13)
Received ECMO	7 (20%)	9 (24%)	14 (41%)	3 (11%)
Median days of ECMO (IQR)	10 (9·5) n = 7	13 (23) n = 9	12 (12) n = 14	27 (NA) n = 3
Received RRT	4 (11%)	16 (42%)	6 (18%)	6 (22%)
Influenza type			NA	NA
Influenza A	31 (89%)	32 (84%)		
Influenza B	4 (11%)	6 (16%)		
Median days ICU stay (IQR)	14 (15)	20 (41)	31 (38)	23 (31)
Median days hospital stay (IQR)	31 (30)	33 (57)	47 (56)	35 (53)
Died in hospital	12 (34%)	19 (50%)	6 (18%)	11 (41%)

** EORTC/MSGERC host factors as described by Donnelly et al*[20]

BAL: bronchoalveolar lavage; BMI: body mass index; COPD: chronic obstructive pulmonary disease; CS: corticosteroids; EORTC: European Organisation for Research and Treatment of Cancer; HSCT: hematopoietic stem cell transplantation; ICU: intensive care unit; MSGERC: Mycoses Study Group Education and Research Consortium; MV: mechanical ventilation.

Supplementary Table 2. Characteristics of aspergillosis diagnosis and treatment in IAPA and CAPA patients with nCounter analyses.

	IAPA (n = 38)	CAPA (n = 27)
Probable aspergillosis*	29	24
Proven aspergillosis*	9	3
Positive BAL culture	23 (61%)	15 (56%)
BAL GM ≥ 1·0	34 (92%) n = 37	26 (96%) n = 27
Median highest BAL GM value throughout ICU stay (IQR)	4·9 (4·2) n = 37	4·7 (4·0) n = 27
Serum GM ≥ 0.5	9 (27%) n = 33	1 (4%) n = 27
Received antifungal therapy for aspergillosis	34 (89%)	27 (100%)
Median days between ICU admission and index BAL with arguments for IPA (IQR)	2·5 (7·3)	5·3 (9·0)

***** *According to the 2020 IAPA consensus criteria[1] and the 2020 CAPA ECMM/ISHAM criteria[2]*

Supplementary Table 3. Clinical characteristics concerning study BAL sampling of included patients with nCounter analyses.

	Influenza-only (n = 35)	IAPA (n = 38)	COVID-19-only (n = 34)	CAPA (n = 27)
Median days between hospital admission and study BAL (IQR)	4·0 (8·0)	5·5 (7·0)	6·8 (6·2)	9 (11)
Median days between ICU admission and study BAL (IQR)	1·0 (2·0)	4·5 (8·2)	4·6 (9·4)	5·3 (9·0)
Median days between start MV and study BAL (IQR)	1·0 (2·0) n = 33	2 (5·0) n = 32	3·5 (7·0) n = 34	3·0 (8·0) n = 27
CS (daily dose ≥20 mg prednisone equivalent) in 48h before study BAL	14 (40%)	17 (45%)	23 (68%)	17 (63%)
Tocilizumab before study BAL	0	0	1 (3%)	0
Anakinra before study BAL	0	0	0	0
Number of patients in whom study BAL = first BAL with arguments for IPA*	NA	34 (89%)	NA	27 (100%)

** For the 4 patients in whom the study BAL sample was not the first BAL sample with arguments for IPA, the BAL sample was taken at 1 day (n=2), 3 days (n=1) and 4 days (n=1) after the first BAL sample with arguments for IPA.*

Supplementary Table 4. Clinical characteristics of included patients with protein analyses (n=162).

	Influenza-only (n = 52)	IAPA (n = 40)	COVID-19-only (n = 38)	CAPA (n = 32)
Mean age – years (SD)	60 (14)	61 (14)	61 (11)	69 (10)
Male sex	26 (50%)	26 (65%)	28 (74%)	29 (91%)
Median BMI (IQR)	26 (7·8)	26 (7·8)	31 (11)	28 (10)
Diabetes mellitus	12 (23%)	7 (18%)	17 (45%)	12 (38%)
Liver cirrhosis	1 (2%)	2 (5%)	0	0
COPD	6 (12%)	11 (28%)	2 (5%)	5 (16%)
EORTC/MSGERC host factor*	14 (27%)	16 (40%)	0	4 (13%)
Hematologic malignancy	5 (10%)	4 (10%)	0	1 (3%)
Allogeneic HSCT	3 (6%)	2 (5%)	0	0
Solid organ transplant	6 (12%)	8 (20%)	0	1 (3%)
Prolonged neutropenia	3 (6%)	3 (8%)	0	0
Prolonged high-dose CS	3 (6%)	2 (5%)	0	1 (3%)
Immunosuppressants	10 (19%)	11 (28%)	0	4 (13%)
Cytotoxic agents	6 (12%)	3 (8%)	0	1 (3%)
Median Charlson Comorbidity Index at ICU admission (IQR)	3 (4)	3 (4)	3 (2)	4 (2)
Median APACHE II score at ICU admission (IQR)	26 (11) n = 50	28 (17) n = 37	24 (9) n = 30	25 (11) n = 28
Received MV	44 (85%)	34 (85%)	37 (97%)	30 (94%)
Median days of MV (IQR)	10 (12)	14 (19)	21 (21) n = 37	16 (14) n = 30
Received ECMO	9 (17%)	9 (23%)	14 (37%)	4 (13%)
Median days of ECMO (IQR)	12 (12)	13 (23)	12 (14) n = 14	23 (41) n = 4
Received RRT	5 (10%)	16 (40%)	5 (13%)	6 (19%)
Influenza type				
Influenza A	41 (79%)	34 (85%)	NA	NA
Influenza B	11 (21%)	6 (15%)	NA	NA
Median days ICU stay (IQR)	14 (14)	19 (39)	27 (32)	24 (32)
Median days hospital stay (IQR)	31 (27)	32 (54)	43 (56)	40 (47)
Died in hospital	15 (29%)	21 (53%)	7 (18%)	11 (34%)

** EORTC/MSGERC host factors as described by Donnelly et al*[20]

BAL: bronchoalveolar lavage; BMI: body mass index; COPD: chronic obstructive pulmonary disease; CS: corticosteroids; EORTC: European Organisation for Research and Treatment of Cancer; HSCT: hematopoietic stem cell transplantation; ICU: intensive care unit; MSGERC: Mycoses Study Group Education and Research Consortium; MV: mechanical ventilation.

Supplementary Table 5. Characteristics of aspergillosis diagnosis and treatment in IAPA and CAPA patients with protein analyses

	IAPA (n = 40)	CAPA (n = 32)
Probable aspergillosis*	30	29
Proven aspergillosis*	10	3
Positive BAL culture	24 (60%)	16 (50%)
BAL GM ≥ 1·0	35 (90%) n = 39	30 (94%) n = 32
Median highest BAL GM value throughout ICU stay (IQR)	4·9 (4·3) n = 39	4·6 (3·8) n = 32
Serum GM ≥ 0·5	9 (23%)	1 (3%) n = 31
Received antifungal therapy for aspergillosis	35 (88%)	32 (100%)
Median days between ICU admission and index BAL with arguments for IPA (IQR)	3·0 (8·0)	5·0 (9·2)

****** *According to the 2020 IAPA consensus criteria*[1] *and the 2020 CAPA ECMM/ISHAM criteria*[2]

Supplementary Table 6. Clinical characteristics concerning study BAL sampling in patients with protein analyses

	Influenza-only (n = 52)	IAPA (n = 40)	COVID-19-only (n = 38)	CAPA (n = 32)
Median days between hospital admission and study BAL (IQR)	4·0 (6·5)	6·0 (6·8)	7·0 (10)	9·0 (11)
Median days between ICU admission and study BAL (IQR)	1·0 (2·0)	3·0 (7·8)	4·0 (9·7)	5·0 (9·2)
Median days between start MV and study BAL (IQR)	1·0 (1·0) n = 44	2·0 (4·0) n = 34	3·0 (5·8) n = 37	3·5 (9·0) n = 30
CS (daily dose ≥20 mg prednisone equivalent) in 48h before study BAL	21 (40%)	17 (43%)	26 (68%)	21 (66%)
Tocilizumab before study BAL	0	0	1 (3%)	0
Number of patients in whom study BAL = first BAL with arguments for IPA*	NA	36 (90%)	NA	32 (100%)

** For the 4 patients in whom the study BAL sample was not the first BAL sample with arguments for IPA, the BAL sample was taken at 1 day (n=2), 3 days (n=1) and 4 days (n=1) after the first BAL sample with arguments for IPA.*

Supplementary Table 7. Characteristics of IAPA and CAPA patients with tracheobronchial biopsies (n=4).

	IAPA patient 1	IAPA patient 2	CAPA patient 1	CAPA patient 2
Age (years)	56	55	38	76
Sex	Male	Male	Male	Male
Diabetes mellitus	0	0	0	0
Liver cirrhosis	0	0	0	0
COPD	0	0	0	0
EORTC/MSGERC host factor*	0	0	0	1
Hematologic malignancy	0	0	0	0
Allogeneic HSCT	0	0	0	0
Solid organ transplant	0	0	0	0
Prolonged neutropenia	0	0	0	0
Prolonged high-dose CS	0	0	0	0
Immunosuppressants	0	0	0	MM*
Cytotoxic agents	0	0	0	0
Charlson Comorbidity Index at ICU admission (SD)	1	1	0	7
APACHE II score at ICU admission (SD)	25	61	NA	NA
Received MV	1	1	1	1
Days of MV	50	16	42	73
Received ECMO	1	1	0	0
Days of ECMO	10	5	0	0
Received RRT	1	1	1	1
Influenza type				
Influenza A	1	1	NA	NA
Influenza B	0	0	NA	NA
Days ICU stay	51	13	45	80
Days hospital stay	54	21	50	145
Died in hospital	1	1	0	0
Positive BAL culture	1 (*A.fumigatus*)	1 (*A.fumigatus*)	1 (*A.fumigatus*)	1 (*A.fumigatus*)
BAL GM ≥ 1·0	1	1	1	0
Highest BAL GM value throughout ICU stay	5.4	>6	2.8	0.4
Serum GM ≥ 0.5	1	1	0	0
Received antifungal therapy for aspergillosis	1	1	1	1
Days between ICU admission and index bronchoscopy/BAL with arguments for IPA	10	2	7	3
Days between ICU admission and biopsy	10	5	18	10
Days between start MV and biopsy	10	5	16	9
CS (daily dose ≥20 mg prednisone equivalent) in 48h before biopsy	1	0	0	1
Tocilizumab before biopsy	0	0	0	0

* *EORTC/MSGERC host factors as described by Donnelly et al*[20]

BAL: bronchoalveolar lavage; COPD: chronic obstructive pulmonary disease; CS: corticosteroids; EORTC: European Organisation for Research and Treatment of Cancer; HSCT: hematopoietic stem cell transplantation; ICU: intensive care unit; MM*: mycophenolate mofetil, stopped on ICU admission. MSGERC: Mycoses Study Group Education and Research Consortium; MV: mechanical ventilation.

Supplementary Table 8

IAPA vs. CAPA uncorrected & corrected for corticosteroids*
Overlapping significant DEGs (n = 1)
Downregulated (n = 1): *CXCL1*
Significant DEGs unique to uncorrected comparison (n = 10)
Downregulated (n = 10): *IL1B; BID; CXCL8; CEBPB; CCL4; TXN; TYROBP; MAP1LC3B; HIST2H2AA3; LTB*

** Corticosteroids defined as a daily dose ≥20 mg prednisone equivalent prior to BAL sampling*

Supplementary Table 9

IAPA vs. CAPA uncorrected & corrected for corticosteroids* (DEGs of corrected comparison with q-value (BH) <0.07)
Overlapping significant DEGs (n = 9)
Downregulated (n = 9): *CXCL1; IL1B; BID; CXCL8; CEBPB; CCL4; TXN; TYROBP; MAP1LC3B*
Significant DEGs unique to corrected comparison (n = 2)
Downregulated (n = 2): *LGALS3; CSTB*
Significant DEGs unique to uncorrected comparison (n = 2)
Downregulated (n = 2): *HIST2H2AA3; LTB*

** Corticosteroids defined as a daily dose ≥20 mg prednisone equivalent prior to BAL sampling*
This table is added to depict that the loss of DEGs for IAPA vs. CAPA when correcting for corticosteroids prior to BAL sampling is probably due to reduction of power, as most DEGs of the uncorrected comparison have BH q-values between 0.05 and 0.07 after correction for corticosteroids.

Supplementary Table 10

Influenza-only vs. COVID-19-only uncorrected & corrected for corticosteroids*
Overlapping significant DEGs (n = 67)
Downregulated (n = 58): *CXCL8; CCL4; NFKBIA; CCL3L1; ALOX5AP; DUSP1; S100A9; TNFAIP3; SOCS3; CCL20; GADD45B; IL1RN; TREM1; C4A; CCL2; LGALS3; CLIC4; ADORA2A; HLA-DPB1; TRAF1; IL1B; HLA-DRA; EMP1; PRDX3; IGHA; ATF3; KIF20A; ID2; ARF6; BID; TXN; CYR61; TNFRSF8; PDE4A; ITGB1; DUSP6; IGHM; SOCS2; CLEC5A; KLF4; VRK2; BIRC2; COL12A1; CEACAM8; ARHGEF28; IL18; IGHG; TREM2; BIRC3; TPSAB1; SMAD7; RNASE2; SMAD1; MYOD1; SERPINE3; CD4; ICOSLG; ERCC1* **Upregulated (n = 9):** *IRF2; NCAM1; CDH4; IGHD; TLR10; NOX1; BMP8A; AICDA; MMP9*
Significant DEGs unique to corrected comparison (n = 8)
Downregulated (n = 8): *S100A8; CSF3R; FCAR; NAMPT; CD14; PROK2; TRAF6; NRIP3*
Significant DEGs unique to uncorrected comparison (n = 7)
Upregulated (n = 2): *TNFSF10; PSMB9* **Downregulated (n = 5):** *TNF; PIM2; TIMP3; PRDX1; DHRS3*

** Corticosteroids defined as a daily dose ≥20 mg prednisone equivalent prior to BAL sampling*

Supplementary Table 11

IAPA vs. influenza-only uncorrected & corrected for time of sampling related to start MV*
Overlapping significant DEGs (n = 96)
Downregulated (n = 84): *MMP9; CD69; NKG7; CREM; CCL4; GRN; MX1; CTSS; CTSD; PROK2; HIST2H2AA3; VASP; STAT6; HLA-DRB3; CXCR4; RHOG; CXCL2; FPR1; IRF1; TYROBP; LAT2; ISG15; PLAUR; AIF1; TNFRSF1B; SQSTM1; TNFSF10; CD83; MAFB; LAPTM5; CD68; HIST1H1C; LTB4R; LTB; FCAR; CRIP1; HLA-DRA; SELL; IRF7; S100A11; RAB20; INSIG1; NCF2; C5AR1; CSTB; S100A4; CEBPB; FCGR3A; ITGAX; CD163; HIF1A; FCGR2A; S100A10; STAT1; SEMA4A; PSMB9; IFNGR1; HES4; C3AR1; IL1B; STAT5A; TNFRSF1A; LGALS3; CXCL1; EGR3; MX2; CCRL2; CEBPD; STAT2; TAP2; RIN2; CTSA; RHOC; IER3; PTAFR; IDO1; MAP1LC3B; TXN; JAML; NFIL3; IFI16; PSME2; MAP2K2; FPR3* **Upregulated (n = 12):** *EMP1; CYR61; C4A; SERPINE3; SOCS2; PDE4A; KIF20A; CTTNBP2; YES1; TREM2; ICOSLG; NRIP3*
Significant DEGs unique to corrected comparison (n = 3)
Downregulated (n = 3): *STAT3; OSM; CTNNB1*
Significant DEGs unique to uncorrected comparison (n = 28)
Downregulated (n = 14): *CCL3; TLR2; PLAU; SIGLEC5; NFKBIE; CYTIP; CYBB; PTX3; PELI1; CCR1; MIF; CNN2; BMP8A; CDH4* **Upregulated (n = 14):** *RNASE2; PGGT1B; HLA-DOB; IL18; CDC20; VTCN1; SERPINB7; ATF3; TNFRSF8; CCR8; MYOD1; TIMP3; ARHGEF28; ANGPT1*

** MV = mechanical ventilation, dichotomous covariate based on sampling time in relation to start of mechanical ventilation (no MV or ≤48 h of MV at sampling time point; or >48 h of MV at sampling time point)*

Supplementary Table 12

CAPA vs. COVID-19-only uncorrected & corrected for time of sampling related to start MV*
Overlapping significant DEGs (n = 27)
Downregulated (n = 27): *GRN; MAFB; HLA-DRA; PTAFR; TLR2; CD68; HIF1A; CCRL2; CD163; C3AR1; IRF1; CXCR4; HLA-DRB3; HLA-DPB1; CYBB; CD83; CDKN1A; SQSTM1; ITGAX; STAT5A; PELI1; ID2; NKG7; RIN2; CRIP1; NFKBIE; ADGRE5*
Significant DEGs unique to corrected comparison (n = 6)
Downregulated (n = 6): *CD74; RHOG; S100A10; LAPTM5; RAB20; ADORA2A*
Significant DEGs unique to uncorrected comparison (n = 7)
Downregulated (n = 7): *MX1; ISG15; TRAF1; TNF; IRF7; STAT2; IFI16*

** MV = mechanical ventilation, dichotomous covariate based on sampling time in relation to start of mechanical ventilation (no MV or ≤48 h of MV at sampling time point; or >48 h of MV at sampling time point)*

Supplementary Figures

Supplementary Figures legends

Supplementary Figure E1. Study set-up.

Samples were obtained from patients admitted to the ICU with severe influenza, with or without IAPA, and severe COVID-19, with or without CAPA. Two types of bronchoscopically-obtained samples were used: bronchoalveolar lavage (BAL) fluid samples and in vivo tracheobronchial biopsies. BAL fluid samples were used for gene expression and protein level analyses, and biopsies were used for RNAscope and spatial transcriptomics. N-values of patients per disease group with samples used per technique are depicted. Made with aid of Biorender.com.

Supplementary Figure E2. Clinical course of included patients.

Panel (**A**): Swimmer plot showing the clinical course timeline of the IAPA (n = 41) and influenza-only patients (n = 52) and the analyses performed for each patient: BAL nCounter gene expression, BAL protein analyses and/or biopsy RNAscope and spatial transcriptomics (green dot indicates that this has been performed). Panel (**B**): Swimmer plot showing the clinical course timeline of the CAPA (n = 35) and COVID-19-only patients (n = 41) and the analyses performed for each patient: BAL nCounter gene expression, BAL protein analyses and/or biopsy RNAscope and spatial transcriptomics (green dot indicates that this has been performed).

Supplementary Figure E3. Cell type fraction correlations.

Correlograms showing the correlations between the deconvoluted cell fractions as obtained by CIBERSORTx. Panel (**A**) shows the correlogram for all patients, while panels (**B**-**E**) show the correlograms for each disease group apart. Components are hierarchically clustered. Asterisks represent significant correlations (*p-value <0·05, **p-value <0·01, ***p-value <0·001, ****p-value <0·0001; Spearman rank correlation).

Supplementary Figure E4. Heat map of ranked DEGs IAPA vs. influenza-only.

Heat map showing the mean-subtracted normalized log2 expression values of the ranked DEGs of the comparison IAPA vs. influenza-only. Values are shown as group mean. Genes are ranked from negative to positive log2 fold change (break indicates change of direction).

Supplementary Figure E5. Heat map of ranked DEGs CAPA vs. COVID-19-only, IAPA vs. CAPA and influenza-only vs. COVID-19-only.

Heat map showing the mean-subtracted normalized log2 expression values of the ranked DEGs of the comparisons CAPA vs. COVID-19-only (panel (**A**)), IAPA vs. CAPA (panel (**B**)) and influenza-only vs. COVID-19-only (panel (**C**)). Values are shown as group mean. Genes are ranked from negative to positive log2 fold change (break indicates change of direction).

Supplementary Figure E6. Volcano plots and venn diagrams of IAPA vs. CAPA and influenza-only vs. COVID-19-only corrected for corticosteroids (CS).

Panel (**A**): Volcano plot of the comparison IAPA vs. CAPA, corrected for corticosteroid use (with corticosteroids defined as a daily dose ≥20 mg prednisone equivalent prior to BAL sampling). Labeled DEGs are the same as those depicted in the uncorrected comparison in Figure 2C.

Panel (**B**): Venn diagram showing the overlap in DEGs between the uncorrected and corticosteroid-corrected comparison IAPA vs. CAPA.

Panel (**C**): Venn diagram showing the overlap in DEGs between the uncorrected and corticosteroid-corrected comparison IAPA vs. CAPA, when including all DEGs with q-value (BH) < 0·07 for the corrected comparison.

Panel (**D**): Volcano plot of the comparison influenza-only vs. COVID-19-only, corrected for corticosteroid use (with corticosteroids defined as a daily dose ≥20 mg prednisone equivalent prior to BAL sampling). Labeled DEGs are the same as those depicted in the uncorrected comparison in Figure 2D.

Panel (**E**): Venn diagram showing the overlap in DEGs between the uncorrected and corticosteroid-corrected comparison influenza-only vs. COVID-19-only.

Supplementary Figure E7. Volcano plots and venn diagrams of IAPA vs. influenza-only and CAPA vs. COVID-19-only corrected for timing of BAL sample in relation to start of mechanical ventilation (MV).

Panel (**A**): Volcano plot of the comparison IAPA vs. influenza-only, corrected for sampling time in relation to start of mechanical ventilation (no MV or ≤48 h of MV at sampling time point; or >48 h of MV at sampling time point). Labeled DEGs are the same as those depicted in the uncorrected comparison in Figure 2A.

Panel (**B**): Venn diagram showing the overlap in DEGs between the uncorrected and the sampling-timepoint corrected comparison IAPA vs. influenza-only.

Panel (**C**): Volcano plot of the comparison CAPA vs. COVID-19-only, corrected for sampling time in relation to start of mechanical ventilation (no MV or ≤48 h of MV at sampling time point; or >48 h of MV at sampling time point). Labeled DEGs are the same as those depicted in the uncorrected comparison in Figure 2B.

Panel (**D**): Venn diagram showing the overlap in DEGs between the uncorrected and sampling-timepoint corrected comparison CAPA vs. COVID-19-only.

Supplementary Figure E8. Chord plots for ClueGO pathway analysis of IAPA vs. influenza-only, CAPA vs. COVID-19-only, IAPA vs. CAPA and influenza-only vs. COVID-19-only.

Chord plots showing gene ontology terms linked to the downregulated DEGs for IAPA vs. influenza-only, CAPA vs. COVID-19-only, IAPA vs. CAPA and influenza-only vs. COVID-19-only**.** The pathways depicted for each comparison in Figure 2F are shown in the chordplot. *For the comparison IAPA vs. CAPA, DEGs with q-value <0.20 were included to generate the analyses, while DEGs with q-value (BH) < 0·05 were used for the other comparisons.

Supplementary Figure E9. GSEA Reactome analysis of IAPA vs. influenza-only with enrichment and leading-edge subset plots.

Dot plot showing the significant (BH q-value <0·25) pathways of the GSEA Reactome analysis for IAPA vs. influenza-only. The ratio of genes included in the nCounter panel and the genes in the Reactome panel are shown next to the pathway name. Leading-edge subset plots of the pathways depicted in the dot plot are shown.

Supplementary Figure E10. GSEA Reactome analysis of CAPA vs. COVID-19-only with enrichment and leading-edge subset plots.

Dot plot showing the significant (BH q-value <0·25) pathways of the GSEA Reactome analysis for CAPA vs. COVID-19-only. The ratio of genes included in the nCounter panel and the genes in the Reactome panel are shown next to the pathway name. Leading-edge subset plots of the pathways depicted in the dot plot are shown.

Supplementary Figure E11-12. GSEA Reactome analysis of IAPA vs. CAPA with enrichment and leading-edge subset plots.

Dot plot showing the significant (BH q-value <0·25) pathways of the GSEA Reactome analysis for IAPA vs. CAPA. The ratio of genes included in the nCounter panel and the genes in the Reactome panel are shown next to the pathway name. Leading-edge subset plots of the pathways depicted in the dot plot are shown.

Supplementary Figure E13. GSEA Reactome analysis of influenza-only vs. COVID-19-only with enrichment and leading-edge subset plots.

Dot plot showing the significant (BH q-value <0·25) pathways of the GSEA Reactome analysis for influenza-only vs. COVID-19-only. The ratio of genes included in the nCounter panel and the genes in the Reactome panel are shown next to the pathway name. Leading-edge subset plots of the pathways depicted in the dot plot are shown.

Supplementary Figure E14. Several genes normally upregulated in PBMCs 24h after stimulation with *Aspergillus fumigatus* are downregulated in IAPA vs. influenza-only and CAPA vs. COVID-19-only.

Volcano plots (cut-offs BH q-value <0·05 and Log2 fold changes >0·4) showing overlap between the significant DEGs in IAPA vs. influenza-only and CAPA vs. COVID-19-only with the genes upregulated in PBMCs 24h after stimulation with *Aspergillus fumigatus* as described by Bruno et al.[21]

Supplementary Figure E15. BAL protein levels.

Levels of cytokines, chemokines and growth factors per disease are displayed as box plots with whiskers set from minimum to maximum, with individual points shown. Q-values calculated using Kruskall-Wallis test with follow-up Benjamini-Krieger-Yekutieli (BKY). Only statistics for comparisons IAPA vs. influenza-only, CAPA vs. COVID-19-only, IAPA vs. CAPA and influenza-only vs. COVID-19-only are shown. Only significant q-values (BKY) are shown.

Supplementary Figure E16. Correlogram of all BAL proteins and correlogram of interferons and interferon-related proteins, with BAL expression of the corresponding gene and CIBERSORTx-derived cell fractions for the latter

Panel (**A**): Correlogram showing the correlations between all assessed BAL proteins. Panel (**B**): Correlogram of interferons and interferon-related proteins, with their respective gene expression and CIBERSORTx-derived cell fractions.

Components are hierarchically clustered. Asterisks represent significant correlations (*p-value <0·05, **p-value <0·01, ***p-value <0·001, ****p-value <0·0001; Spearman rank correlation).

Supplementary Figure E17. Correlogram of TNF-related proteins and other proteins, and correlogram of interleukins, with the BAL expression of the corresponding gene and CIBERSORTx-derived cell fractions.

Panel (**A**): Correlogram of TNF-α-related and other proteins, with their respective gene expression and CIBERSORTx-derived cell fractions. Panel (**B**): Correlogram of interleukins, with their respective gene expression and CIBERSORTx-derived cell fractions.

Components are hierarchically clustered. Asterisks represent significant correlations (*p-value <0·05, **p-value <0·01, ***p-value <0·001, ****p-value <0·0001; Spearman rank correlation).

Supplementary Figure E18. Correlogram of chemokines, and correlogram of growth factors, with the BAL expression of the corresponding gene and CIBERSORTx-derived cell fractions.

Panel (**A**): Correlogram of chemokines, with their respective gene expression and CIBERSORTx-derived cell fractions. Panel (**B**): Correlogram of growth factors, with their respective gene expression and CIBERSORTx-derived cell fractions.

Components are hierarchically clustered. Asterisks represent significant correlations (*p-value <0·05, **p-value <0·01, ***p-value <0·001, ****p-value <0·0001; Spearman rank correlation).

Supplementary Figure E19. Correlogram of major cytokines, corresponding genes and CIBERSORTx-derived cell fractions for IAPA and influenza-only.

Correlogram of the major cytokines with their respective gene expression and CIBERSORTx-derived cell fractions in IAPA (panel (**A**)) and influenza-only (panel (**B**)).

Components are hierarchically clustered. Asterisks represent significant correlations (*p-value <0·05, **p-value <0·01, ***p-value <0·001, ****p-value <0·0001; Spearman rank correlation).

Supplementary Figure E20. Correlogram of major cytokines, corresponding genes and CIBERSORTx-derived cell fractions for CAPA and COVID-19-only.

Correlogram of the major cytokines with their respective gene expression and CIBERSORTx-derived cell fractions in CAPA (panel (**A**)) and COVID-19-only (panel (**B**)).

Components are hierarchically clustered. Asterisks represent significant correlations (*p-value <0·05, **p-value <0·01, ***p-value <0·001, ****p-value <0·0001; Spearman rank correlation).

Supplementary Figure E21. Pathway module score heat maps, correlations between neutrophil scores and pro-inflammatory module scores, and correlation between IFN-α and the respective module score.

Panel (**A**): Heat maps of the genes included in the pathway (type I & II IFN, IL-1β, TNF-α) module scores per disease. Color intensity represents the median z-score as calculated for each gene among all four disease groups using log2 normalized gene counts.

Panel (**B**): Spearman rank correlation between neutrophils scores and IL-1β or TNF-α module scores for all patients. Lines and shades represent the regression lines with 95% confidence interval.

(**C**): Spearman rank correlation between IFN-α levels and the corresponding module score for all patients and for the patients per disease group. Lines and shades represent the regression lines with 95% confidence interval.

Supplementary Figure 22. Tracheobronchial *in vivo* biopsy of CAPA patient 1 and 2.

Panel (**A**): H&E staining of the tracheobronchial biopsy of CAPA patient 1. Panel (**B**): magnified image of H&E staining. Small colored frames depict the regions where respective GeoMx ROIs were selected. Panel (**C**): Grocott-Gomori's methenamine staining of the magnified image. Panel (**D**): ROIs are aligned by a white line. ROI images are from immunohistochemistry (IHC) (cytokeratin = green, CD68 = yellow, CD45 = red, DNA = blue).

Panel (**E**): H&E staining of the tracheobronchial biopsy of CAPA patient 2. Small colored frames depict the regions where respective GeoMx ROIs were selected. Panel (**F**): Grocott-Gomori's methenamine staining of the image. Panel (**G**)**:** ROIs are aligned by a white line. ROI images are from IHC (cytokeratin = green, CD68 = yellow, CD45 = red, DNA = blue).

Supplementary Figure E23. Tracheobronchial *in vivo* biopsy of IAPA patient 1.

Panel (**A**): H&E staining of the tracheobronchial biopsy. Small colored frames depict the regions where respective GeoMx ROIs were selected. Panel (**B**): Grocott-Gomori's methenamine staining of the magnified image. Panel (**C**): ROIs are aligned by a white line. ROI images are from IHC (cytokeratin = green, CD68 = yellow, CD45 = red, DNA = blue).

Supplementary Figure E24. Tracheobronchial *in vivo* biopsy 1 & 2 of IAPA patient 2.

Panel (**A**): H&E staining of the first tracheobronchial biopsy. Panel (**B**): magnified image of H&E staining. Small colored frames depict the regions where respective GeoMx ROIs were selected. Panel (**C**): Grocott-Gomori's methenamine staining of the magnified part. Panel (**D**): ROIs are aligned by a white line. ROI images are colored with IHC (cytokeratin = green, CD68 = yellow, CD45 = red, DNA = blue).

Panel (**E**): H&E staining of the second tracheobronchial biopsy. Panel (**F**): magnified H&E staining. Small colored frames depict the regions where respective GeoMx ROIs were selected. Panel (**G**): Grocott-Gomori's methenamine staining of the magnified part. Panel (**H**): ROIs are aligned by a white line. ROI-images are from IHC (cytokeratin = green, CD68 = yellow, CD45 = red, DNA = blue).

Supplementary Figure E25. Volcano plots of epithelium and inflammatory infiltrate ROIs in IAPA vs. CAPA.

Volcano plot of DEGs comparing respectively epithelium and inflammatory infiltrate ROIs in IAPA vs. CAPA.

Supplementary Figure E26. Enrichment and leading-edge subset plots of GSEA Reactome analysis of IAPA vs. CAPA Epithelium. Upregulated pathways.

Enrichment and leading-edge subset plots derived from the GSEA Reactome analysis of IAPA vs. CAPA Epithelium. The ten upregulated pathways depicted in Figure 5G are shown.

Supplementary Figure E27. Enrichment and leading-edge subset plots of GSEA Reactome analysis of IAPA vs. CAPA Epithelium. Downregulated pathways.

Enrichment and leading-edge subset plots derived from the GSEA Reactome analysis of IAPA vs. CAPA Epithelium. The ten downregulated pathways depicted in Figure 5G are shown.

Supplementary Figure E1

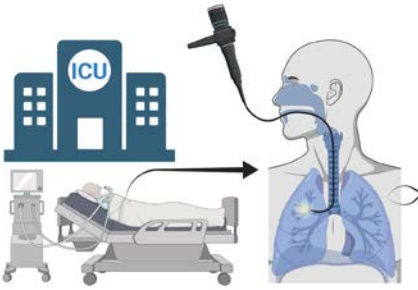

	IAPA	Influenza-only	CAPA	COVID-19-only	Total
Gene expression	38	35	27	34	134
Protein levels	40	52	32	38	162
RNAscope	2		2		4
Spatial transcriptomics					

Supplementary Figure E2

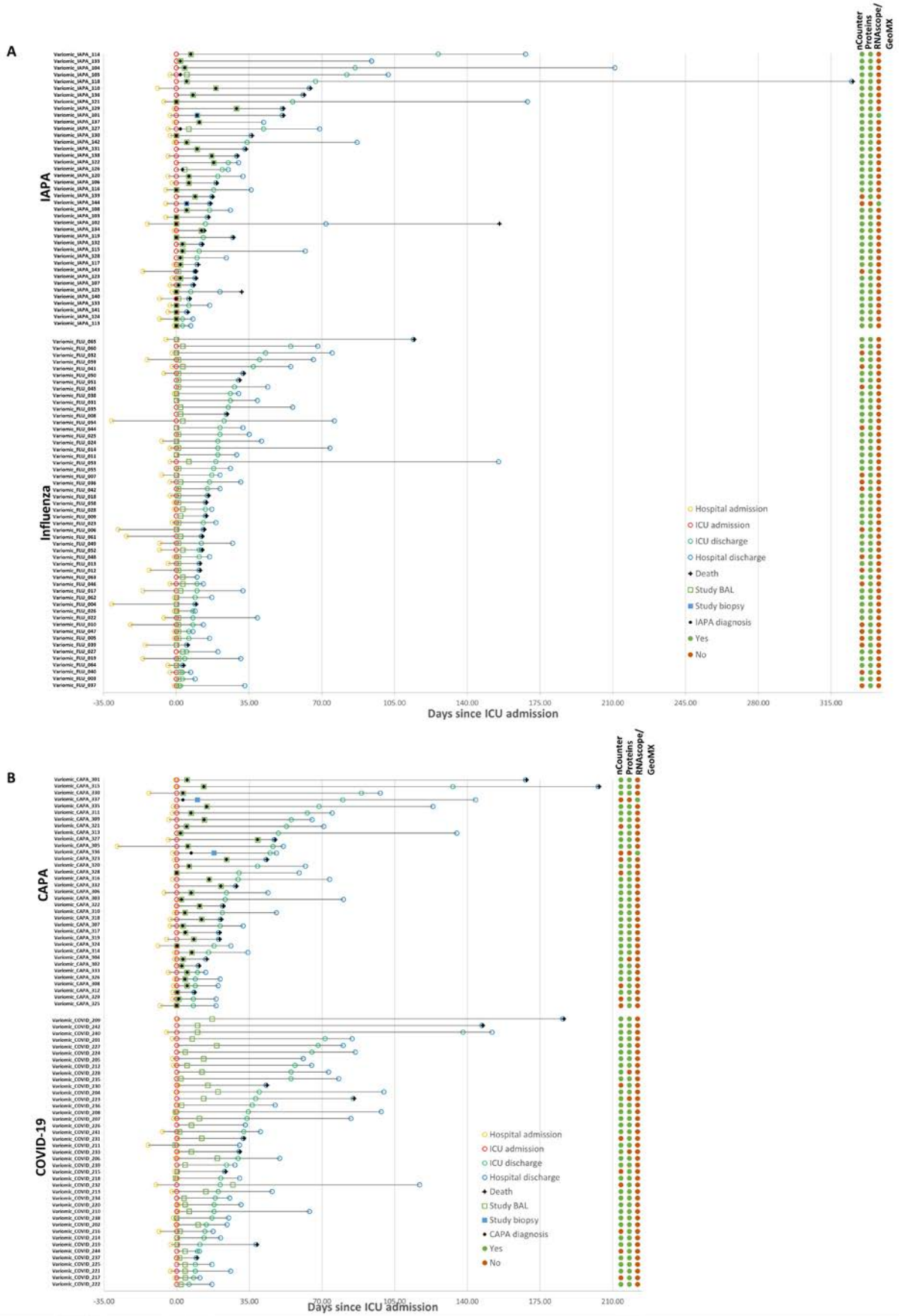

Supplementary Figure E3

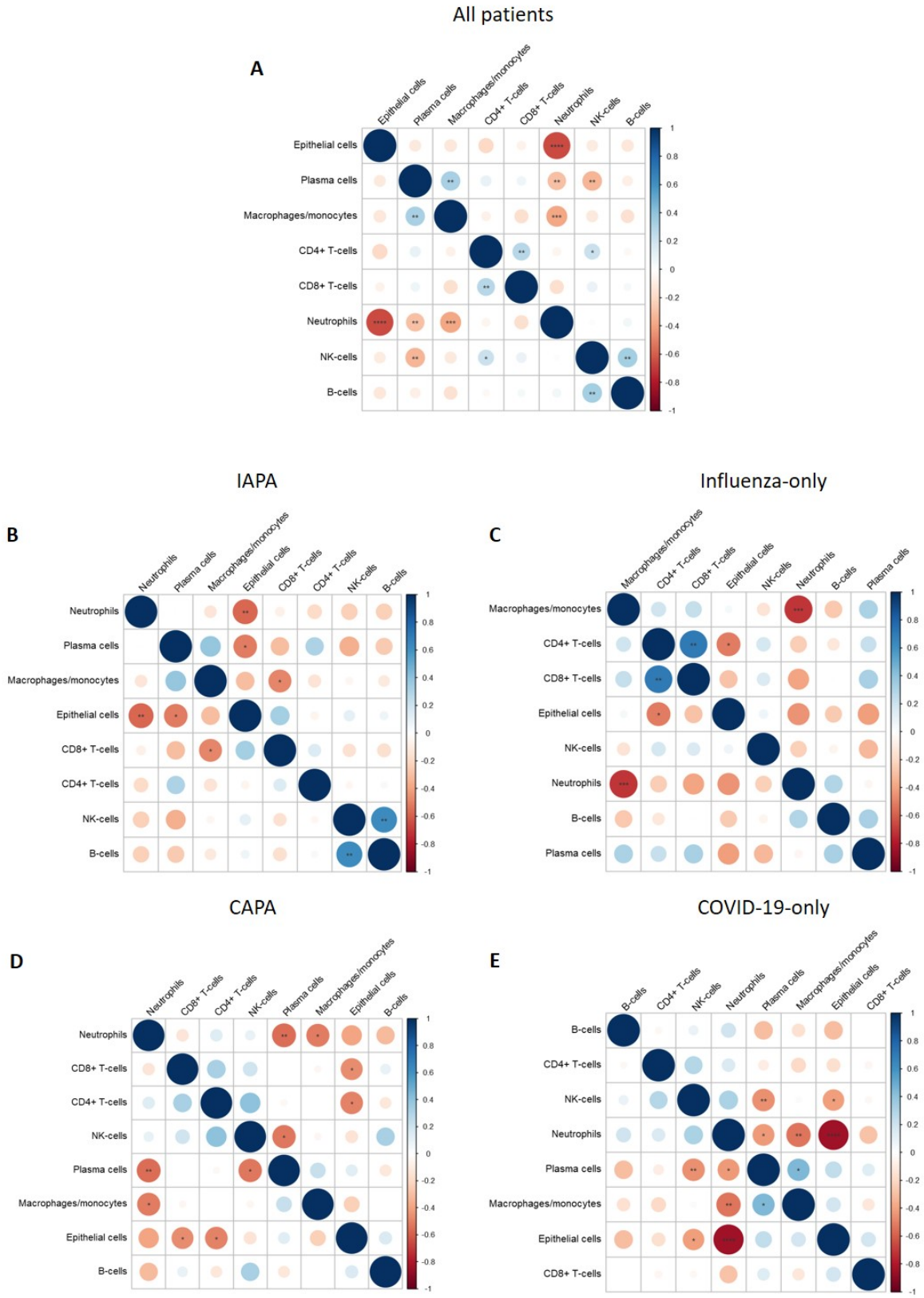

Supplementary Figure E4

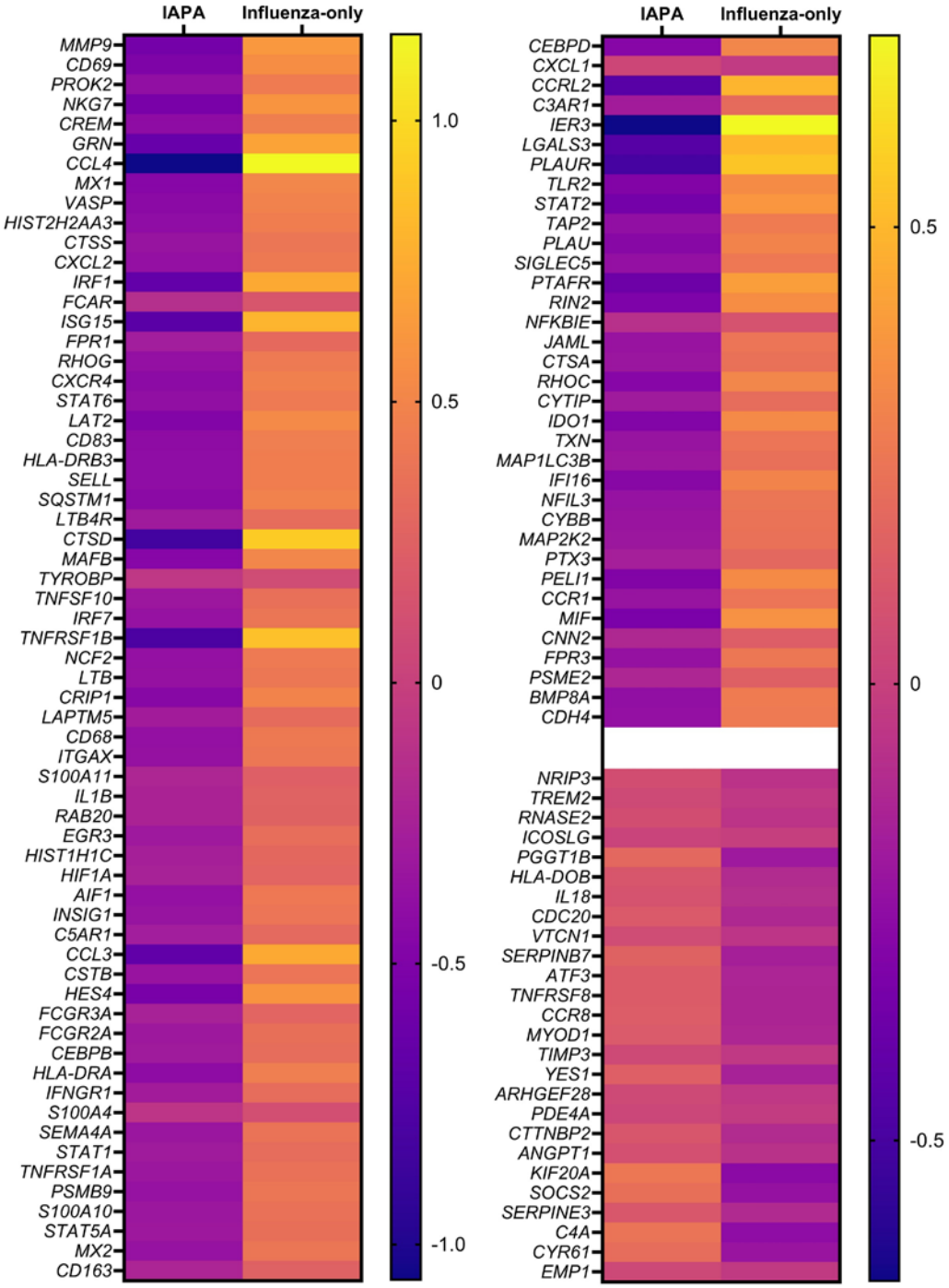

Supplementary Figure E5

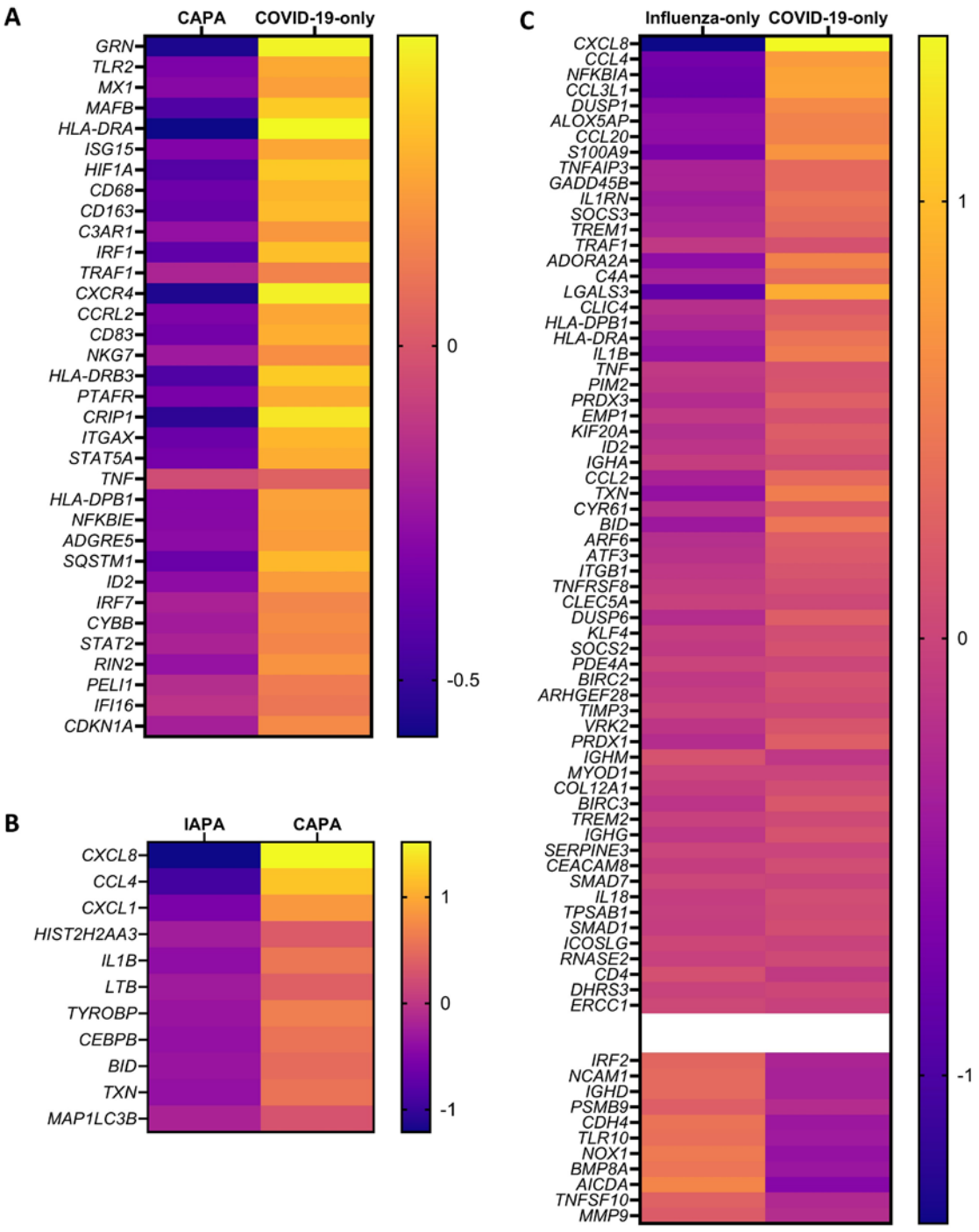

Supplementary Figure E6

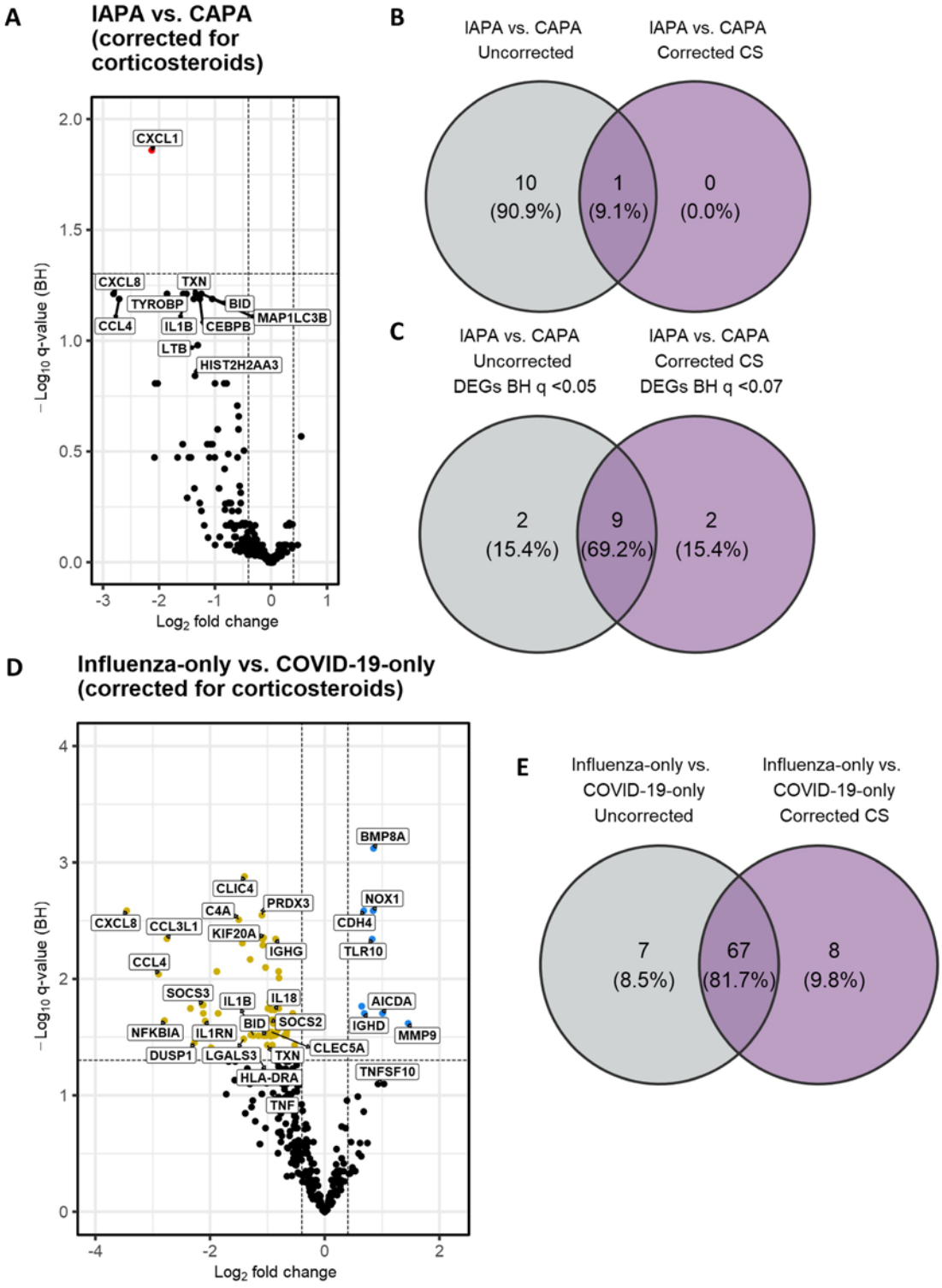

Supplementary Figure E7

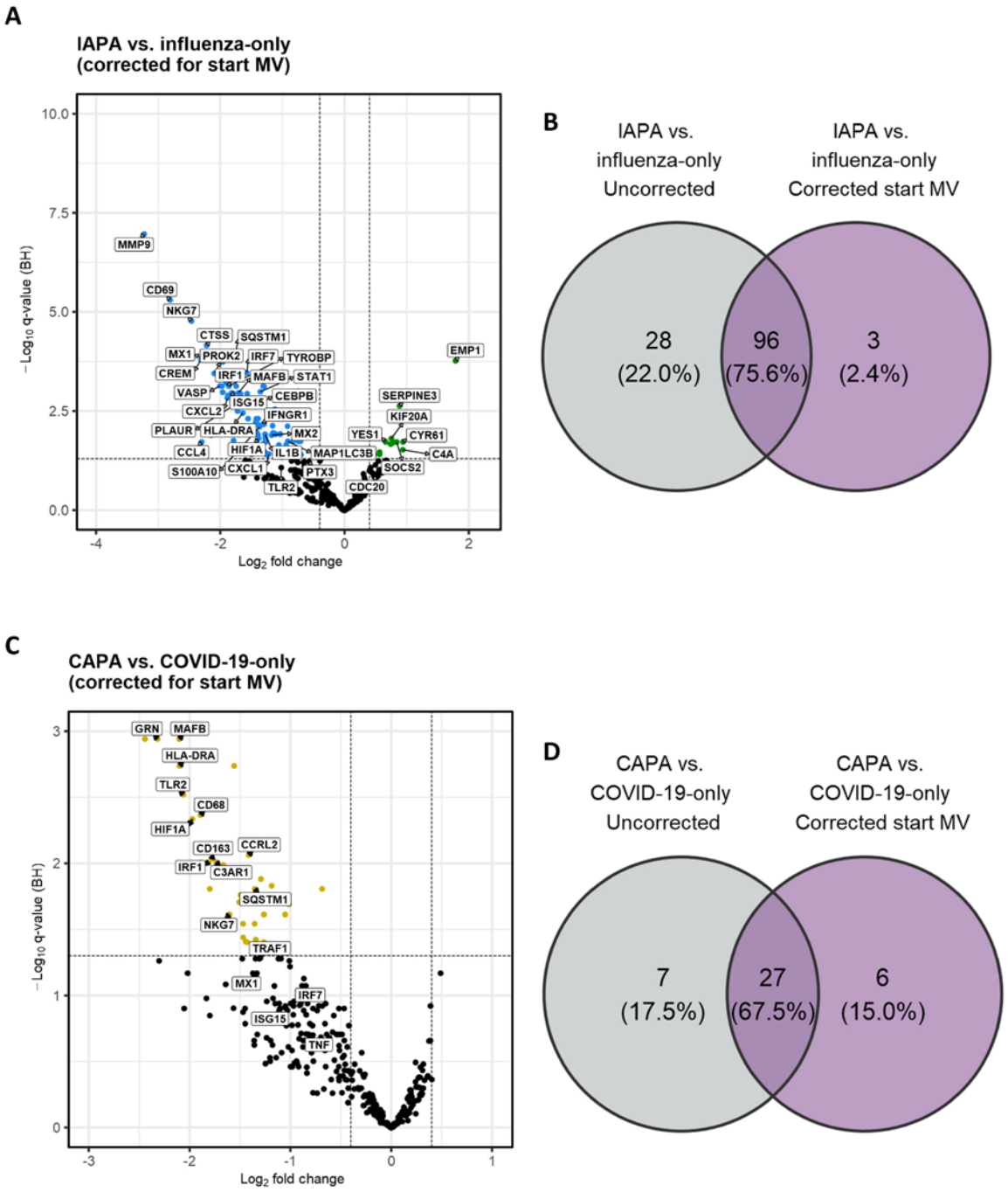

Supplementary Figure E8

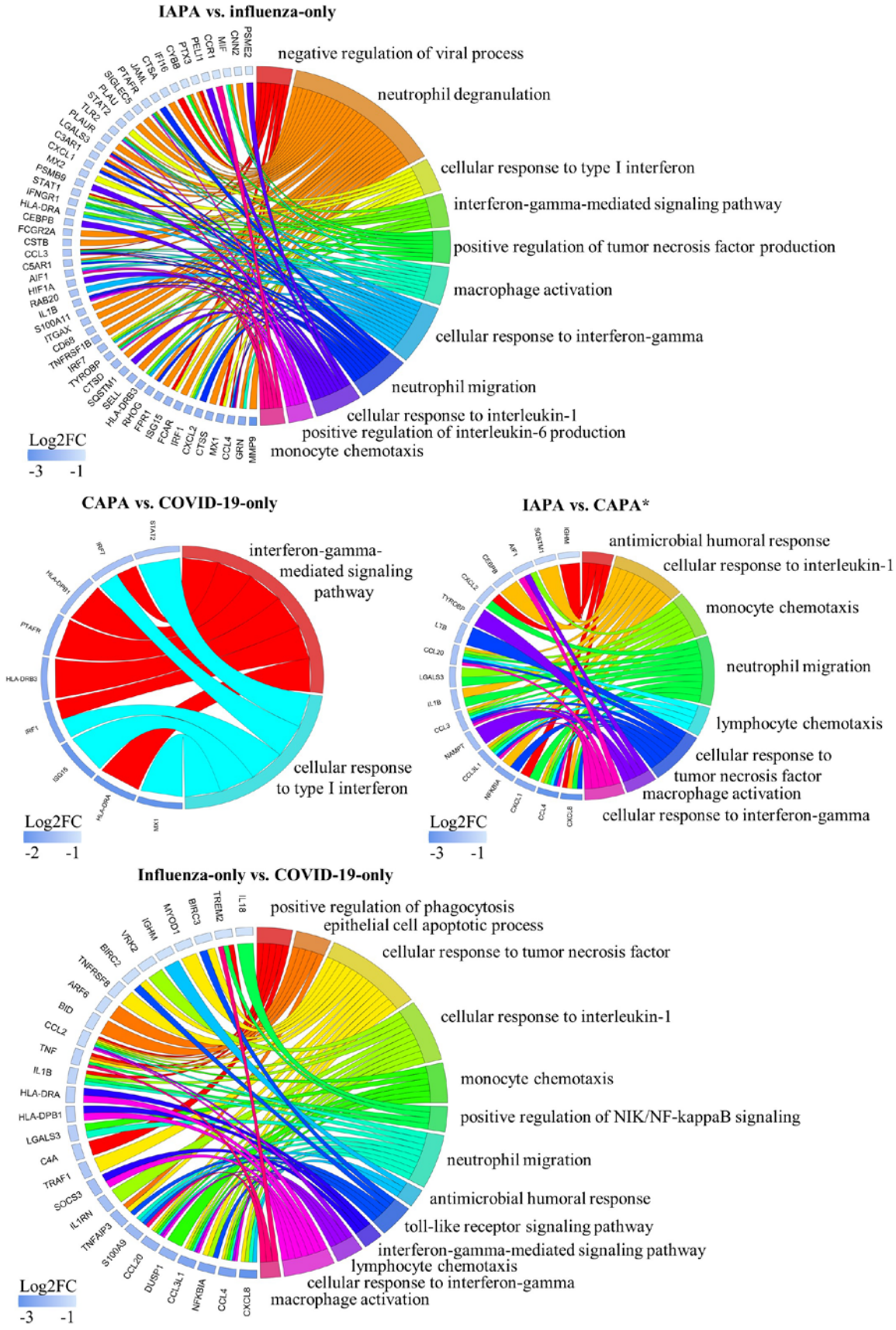

Supplementary Figure E9

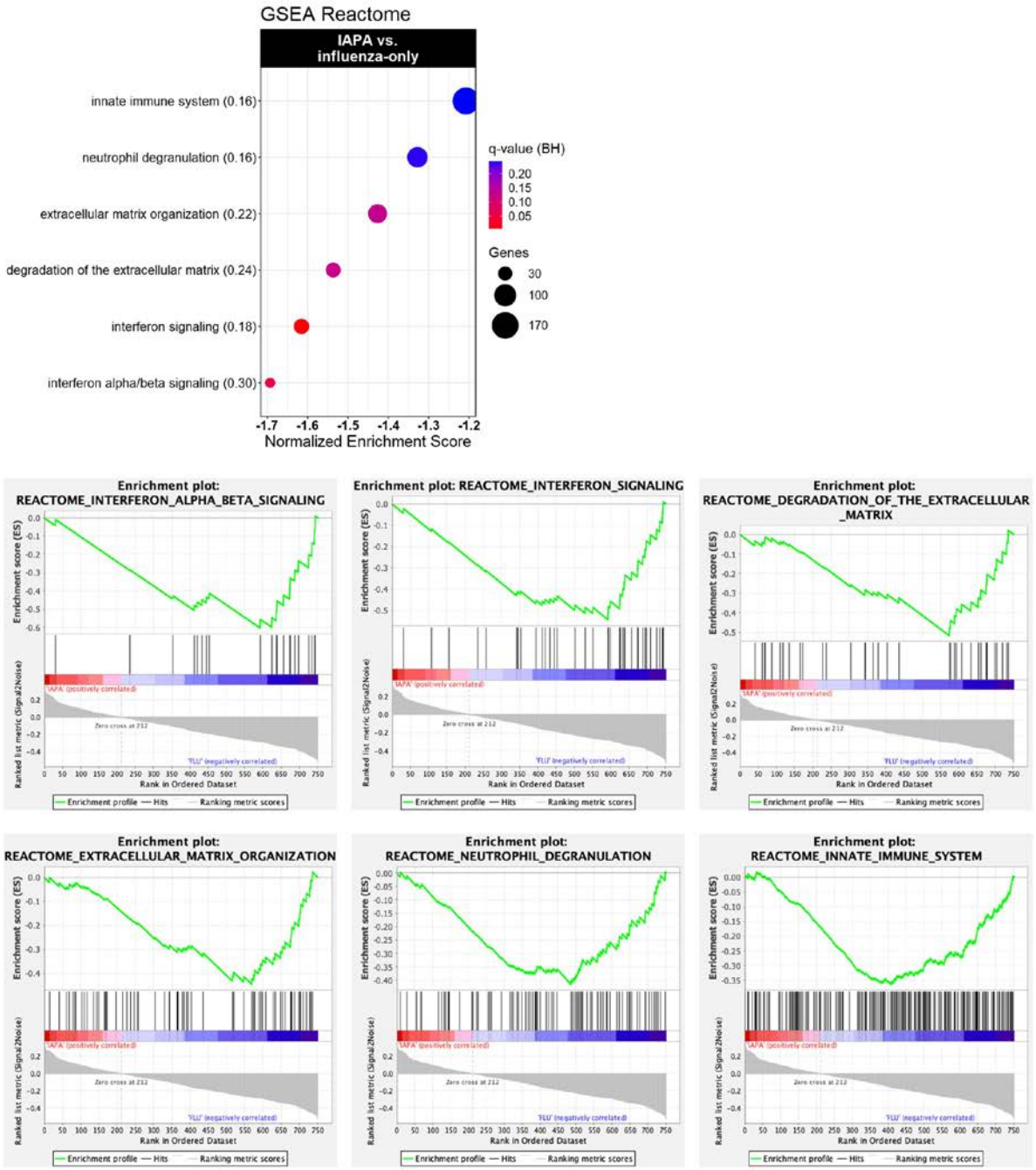

Supplementary Figure E10

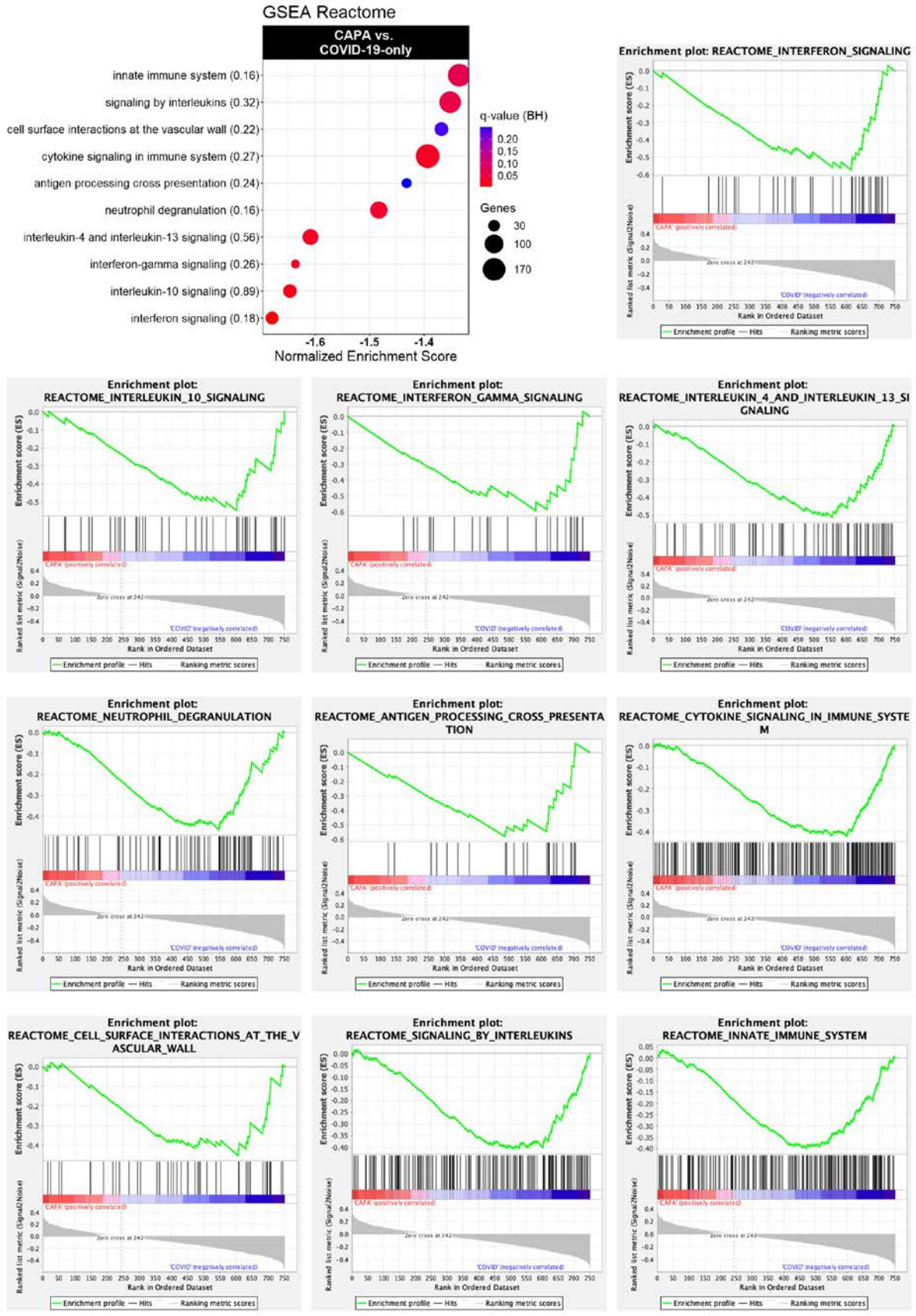

Supplementary Figure E11

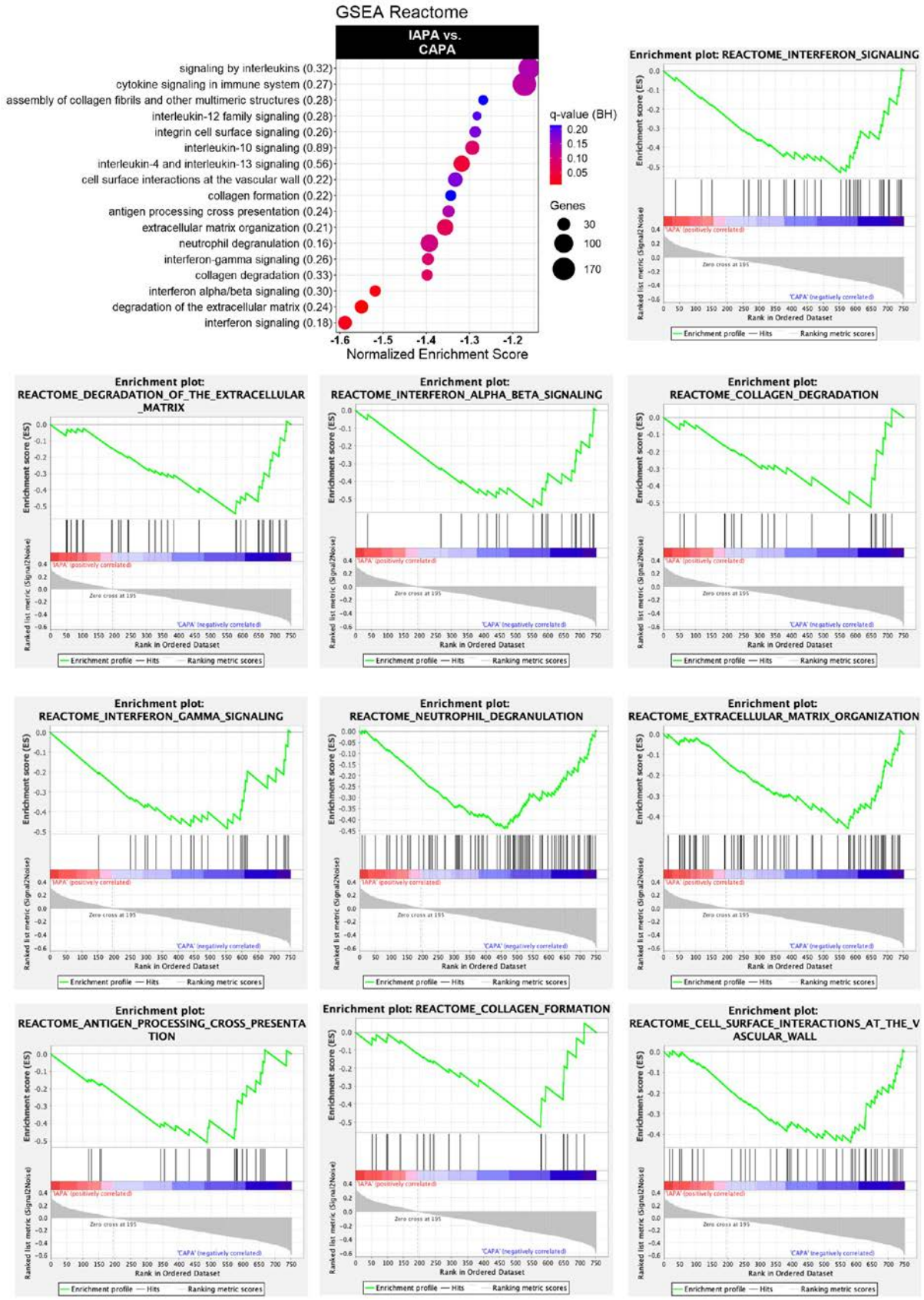

Supplementary Figure E12

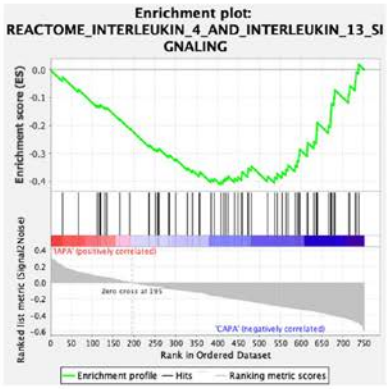

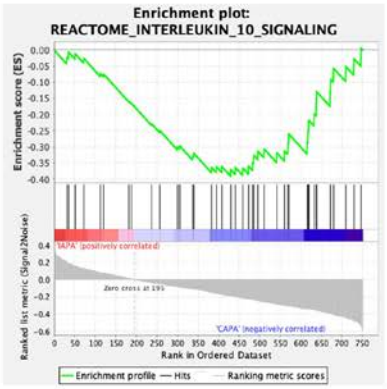

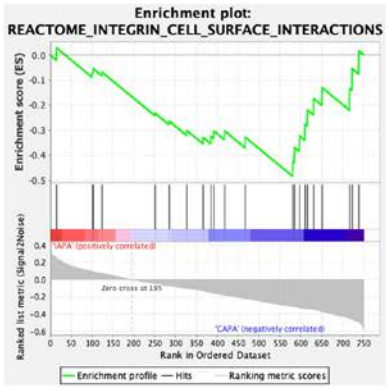

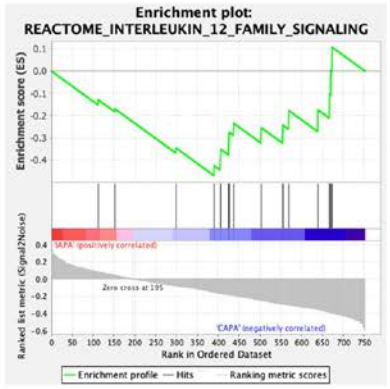

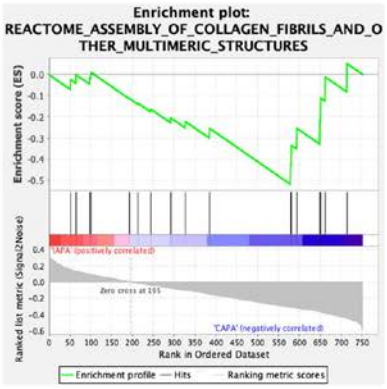

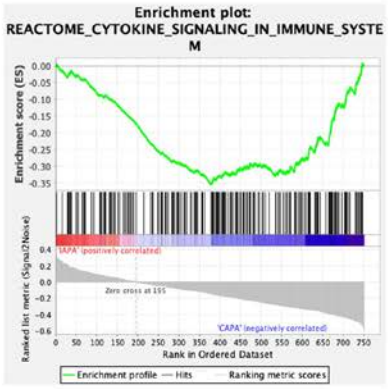

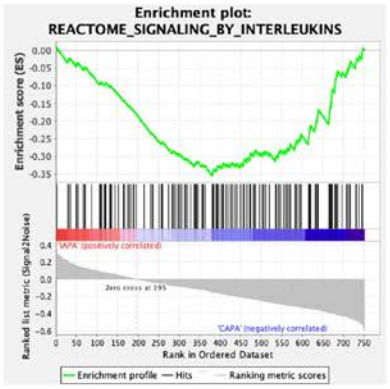

Supplementary Figure E13

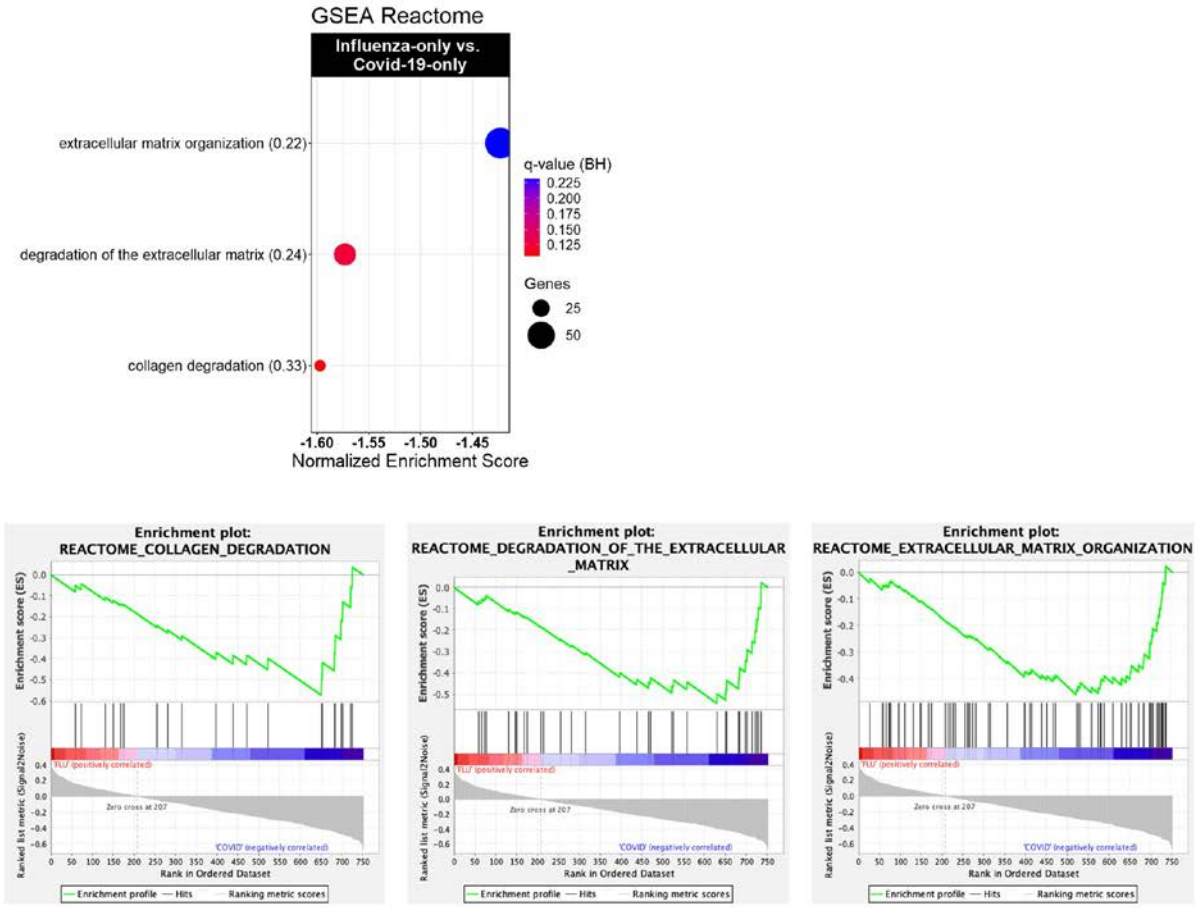

Supplementary Figure E14

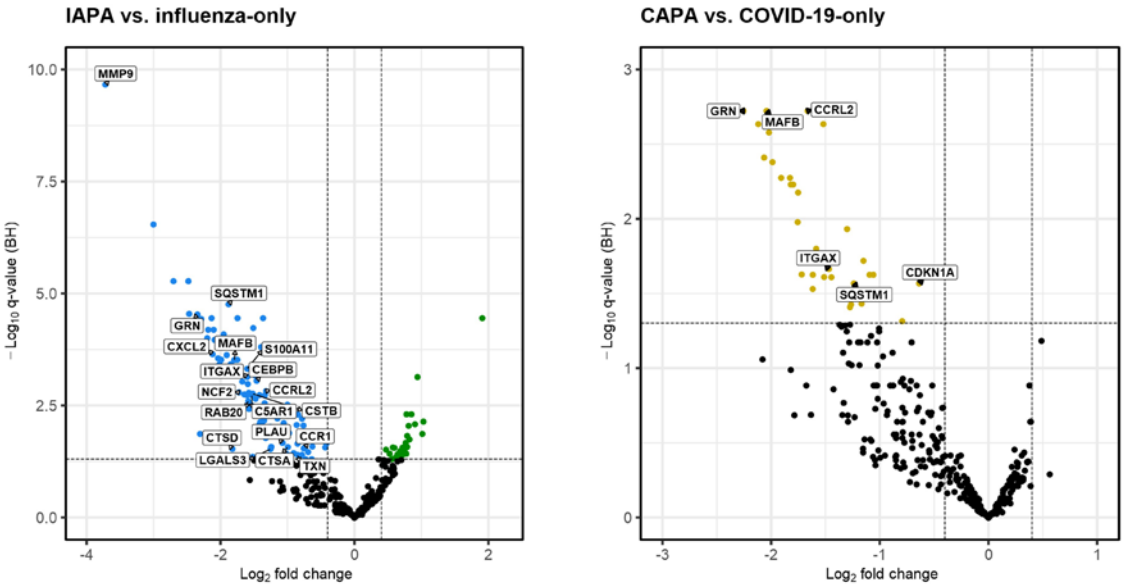

Supplementary Figure E15

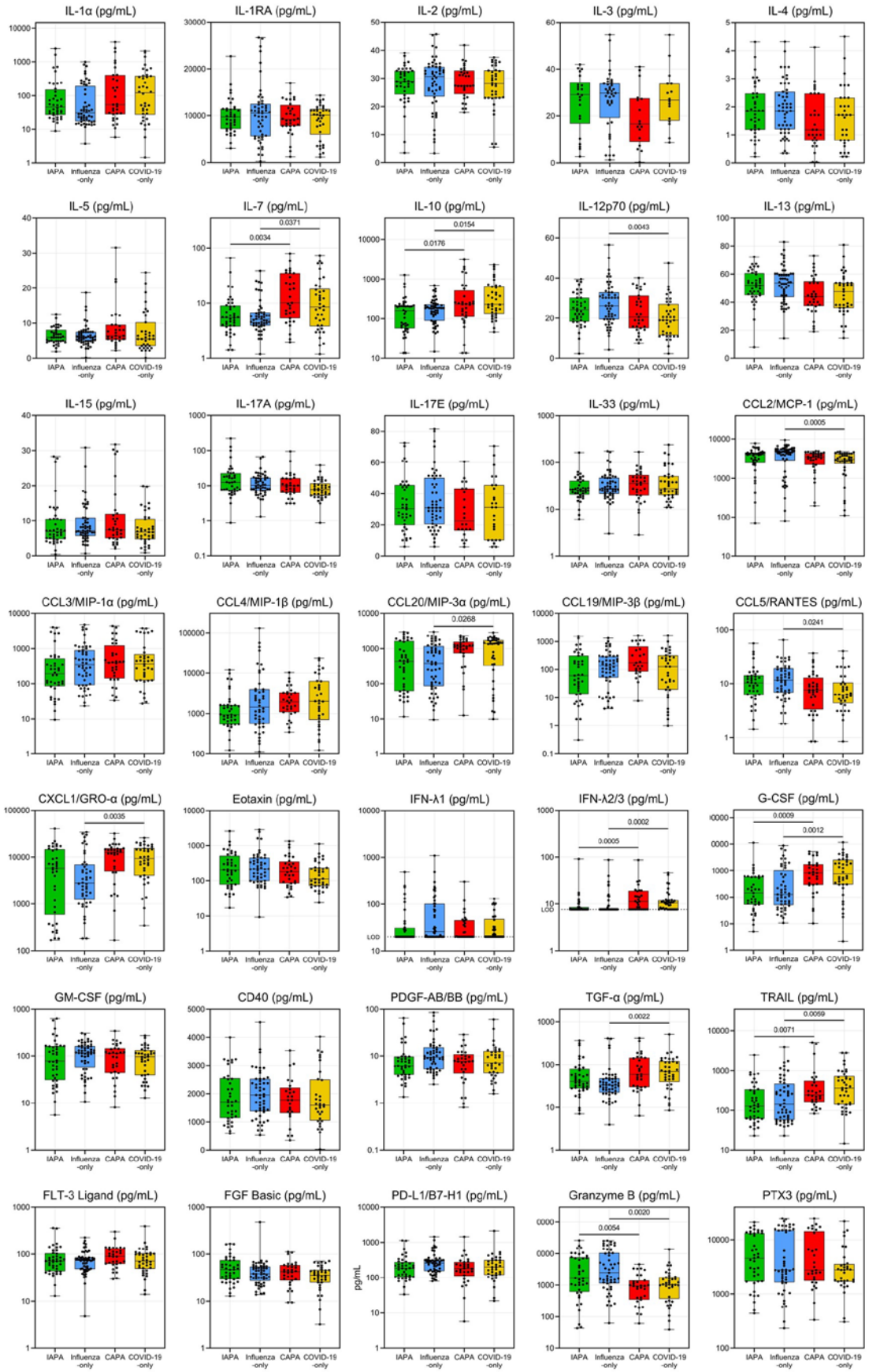

Supplementary Figure E16

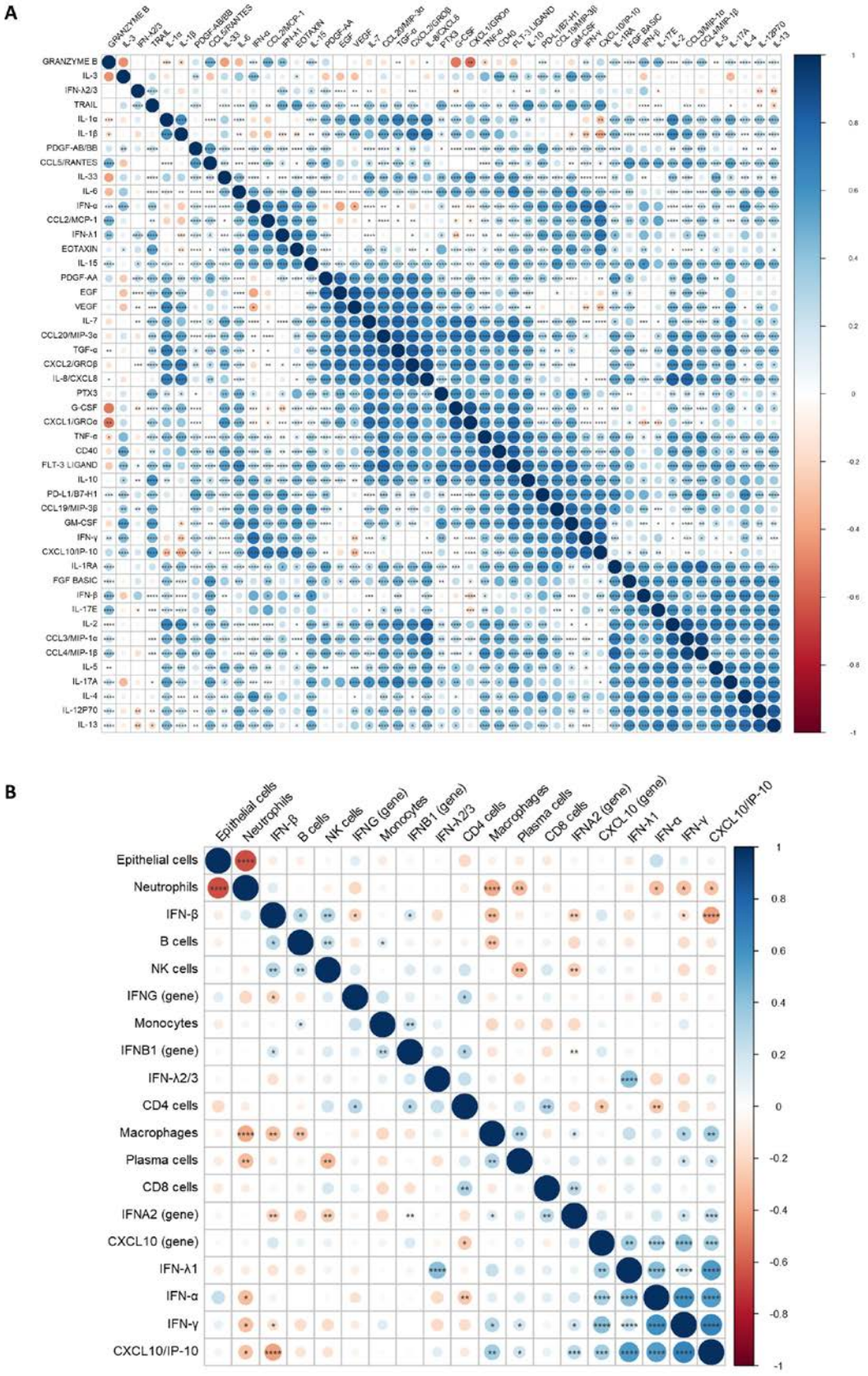

Supplementary Figure E17

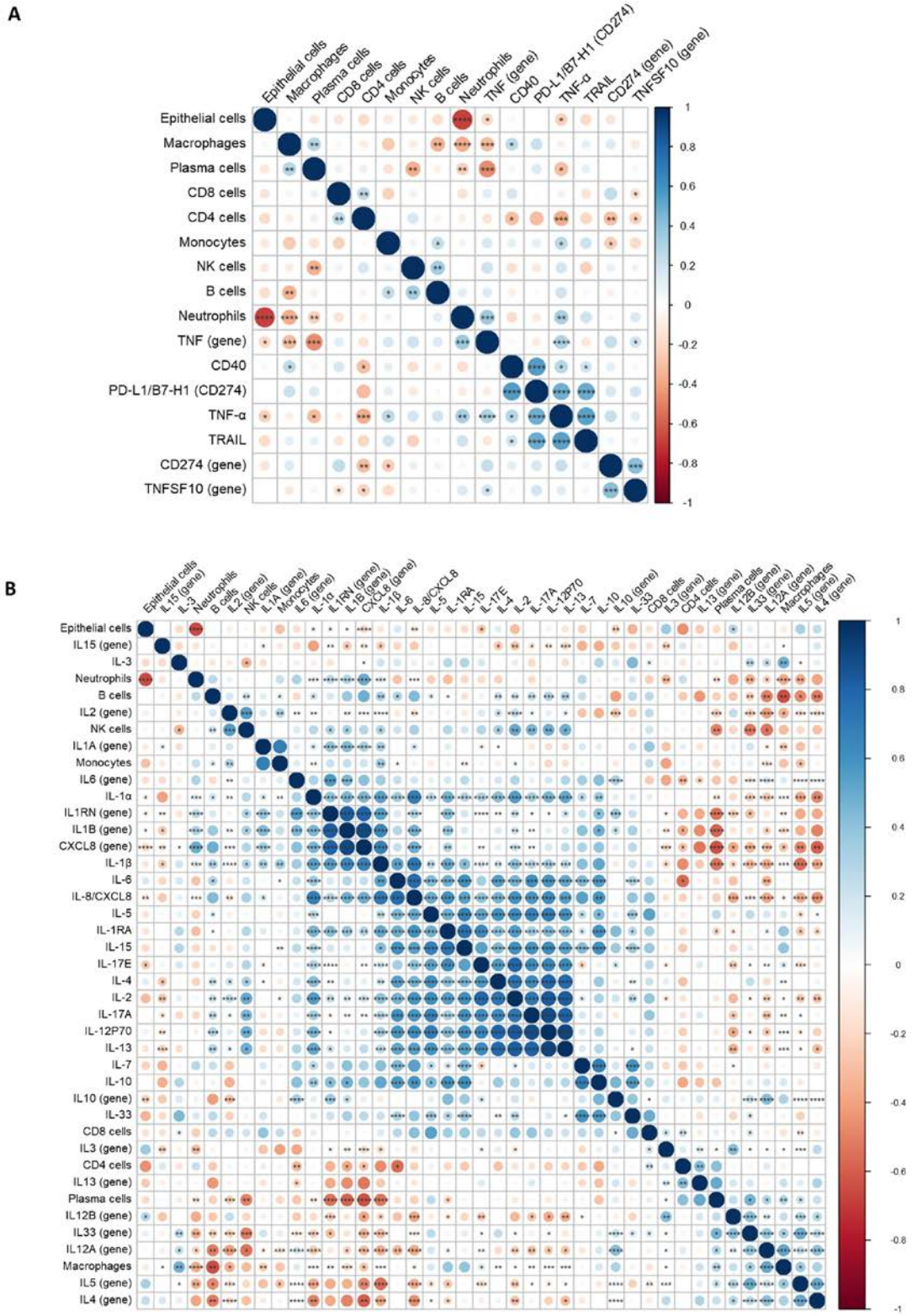

Supplementary Figure E18

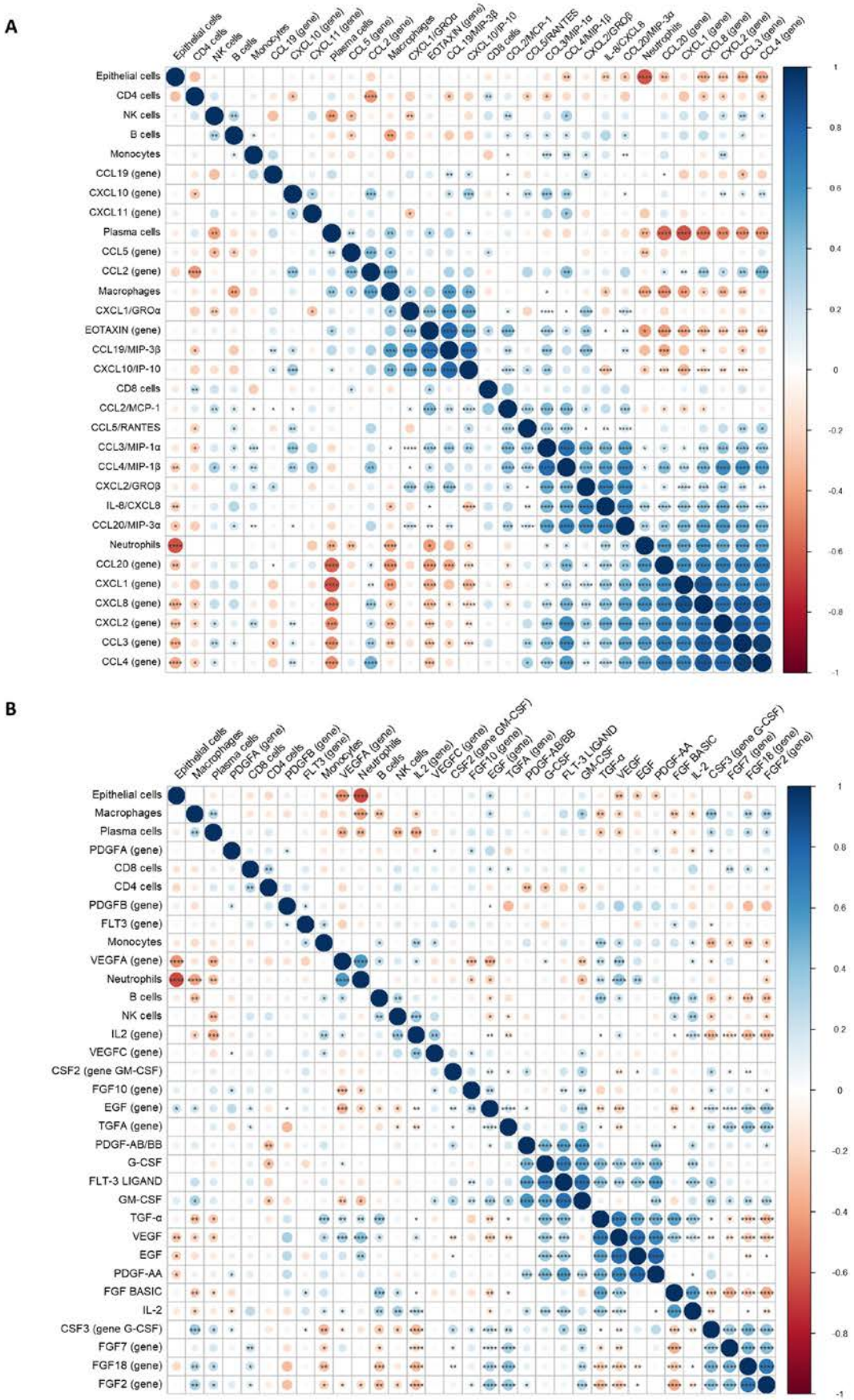

Supplementary Figure E19

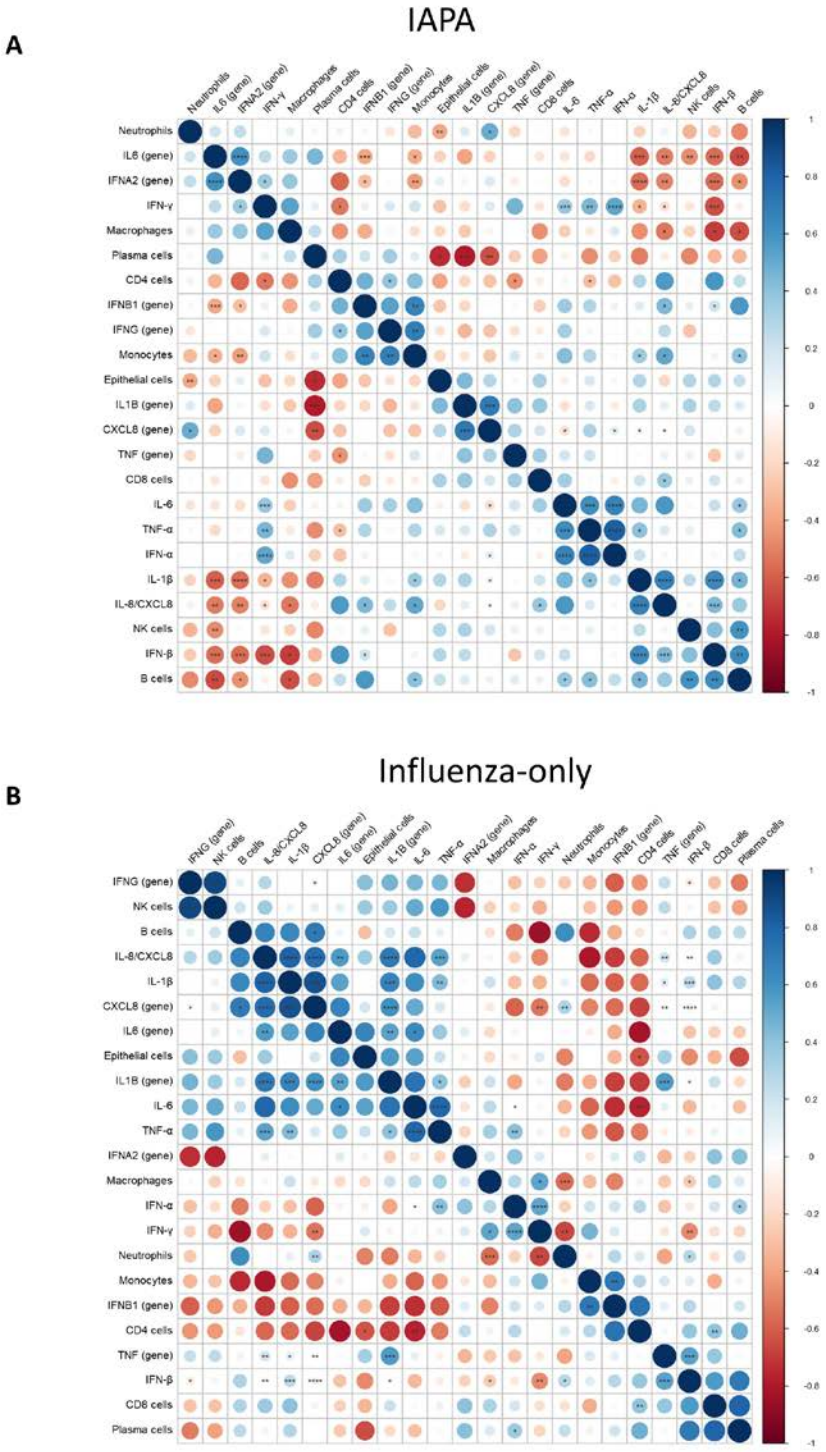

Supplementary Figure E20

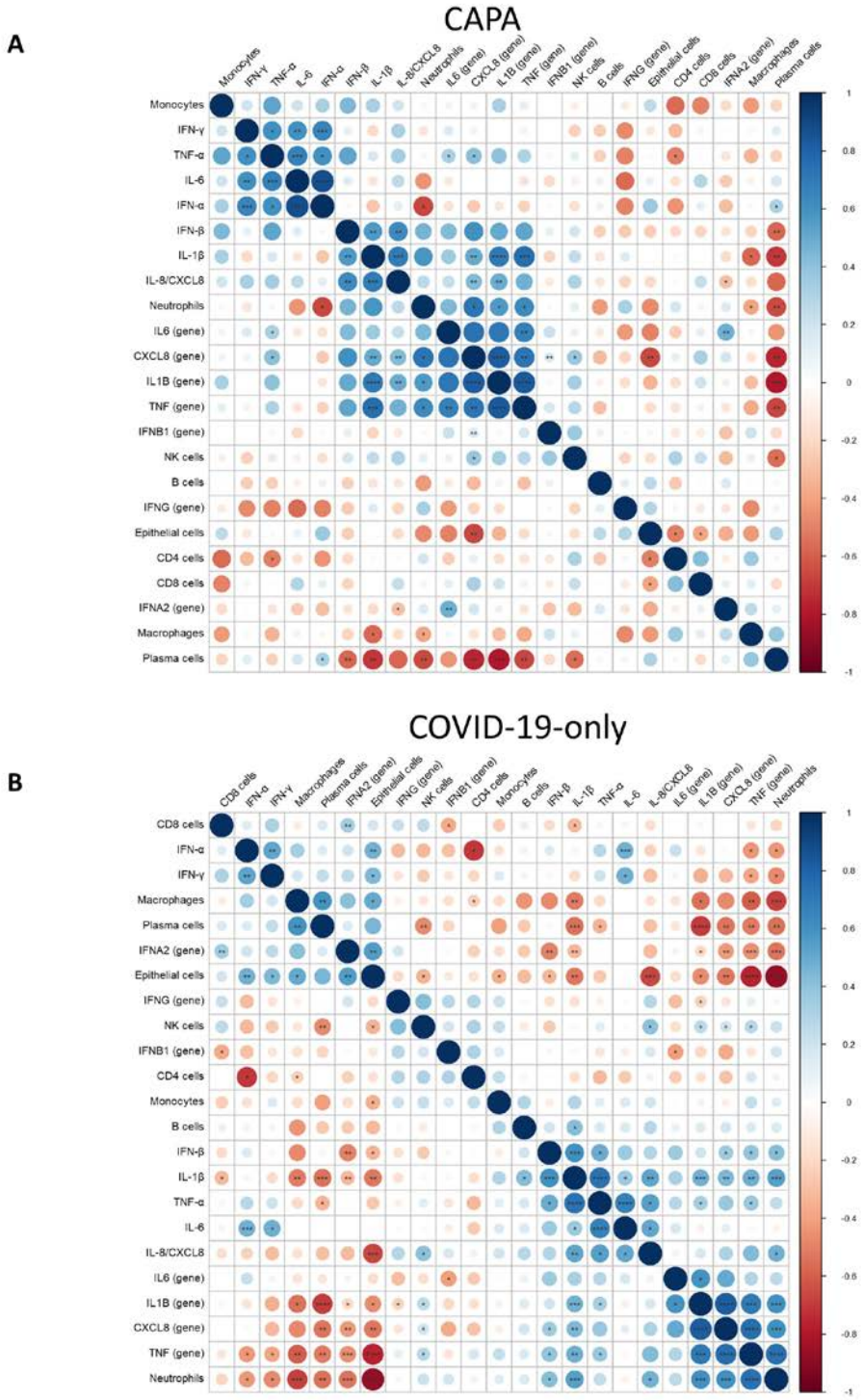

Supplementary Figure E21

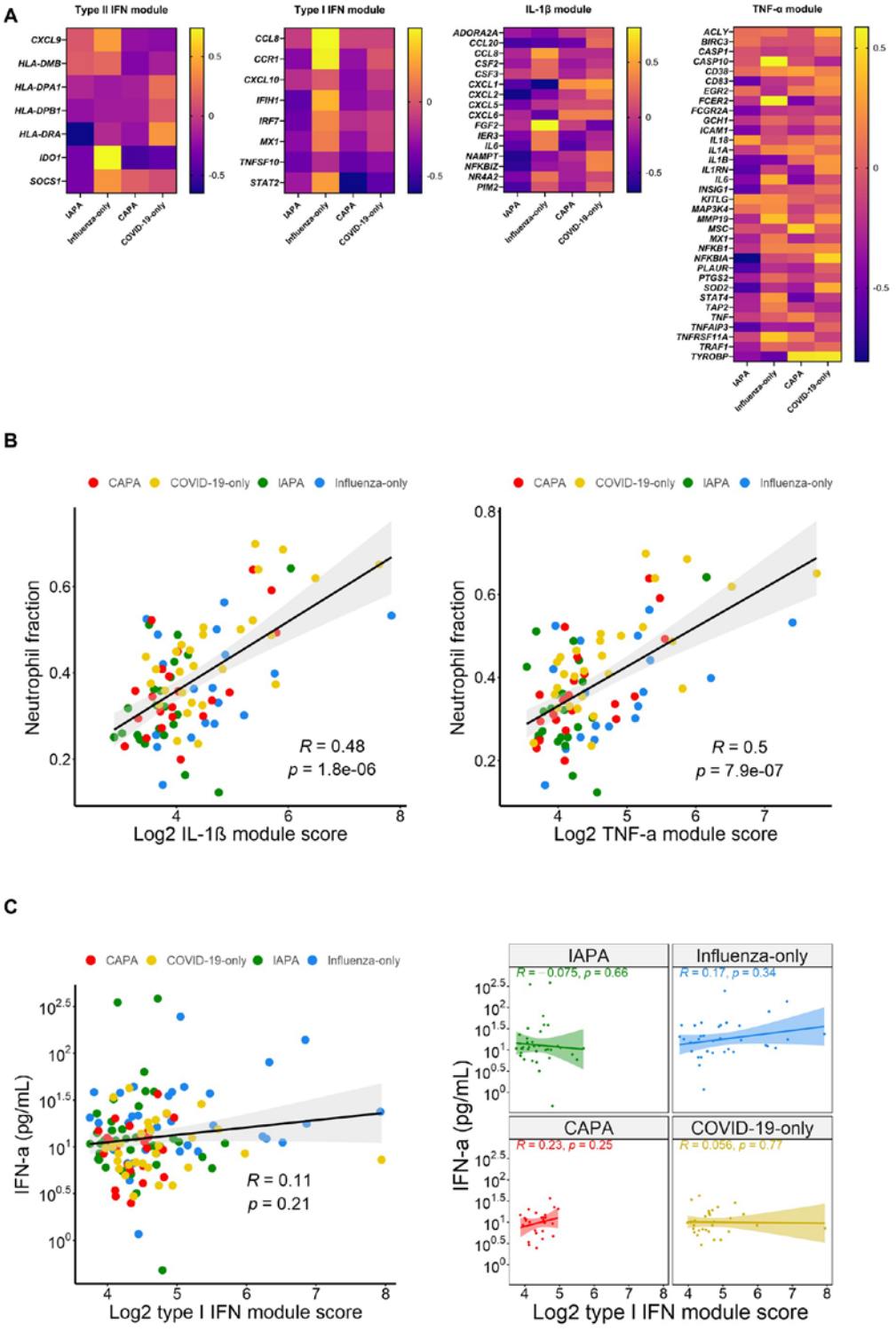

Supplementary Figure E22

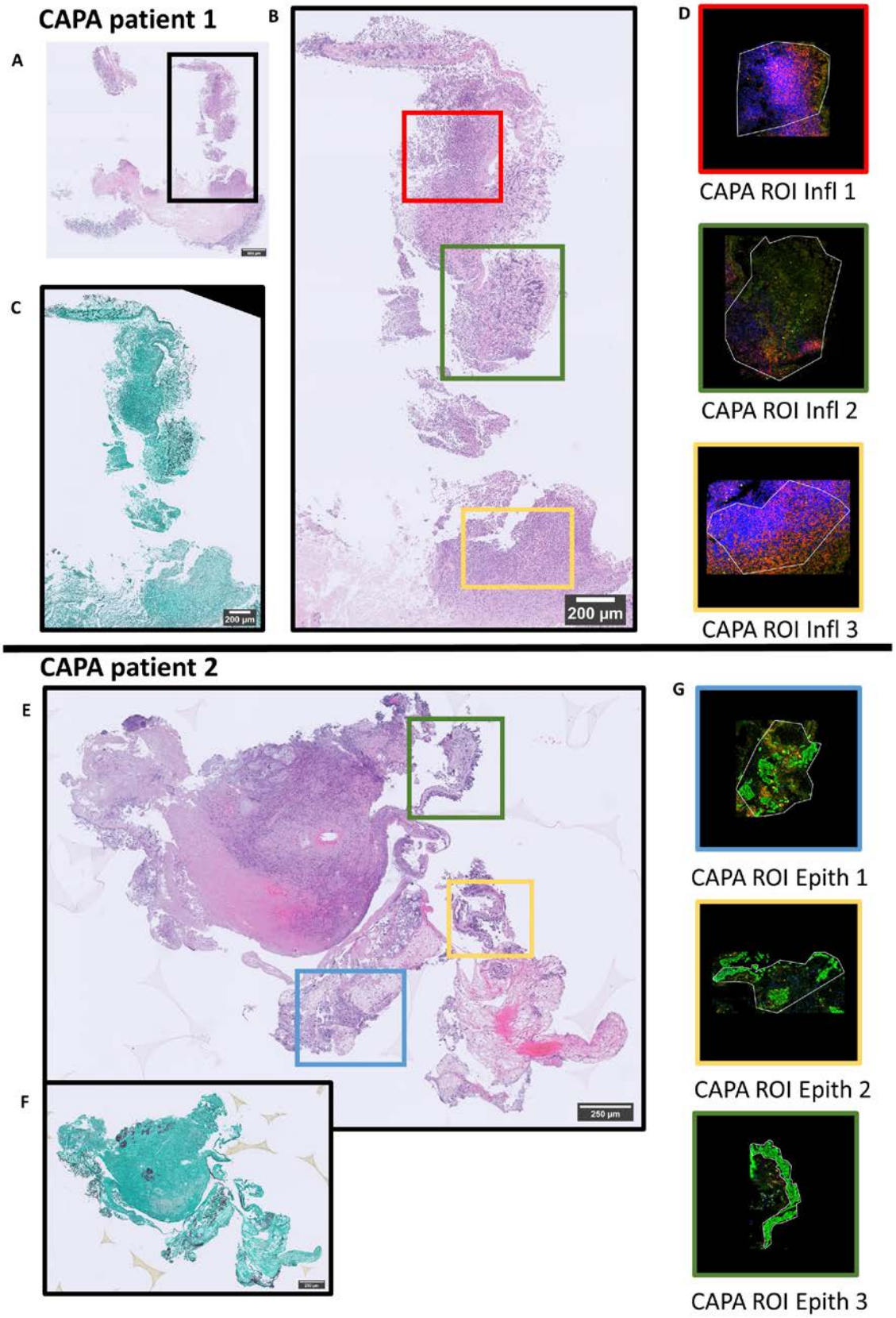

Supplementary Figure E23

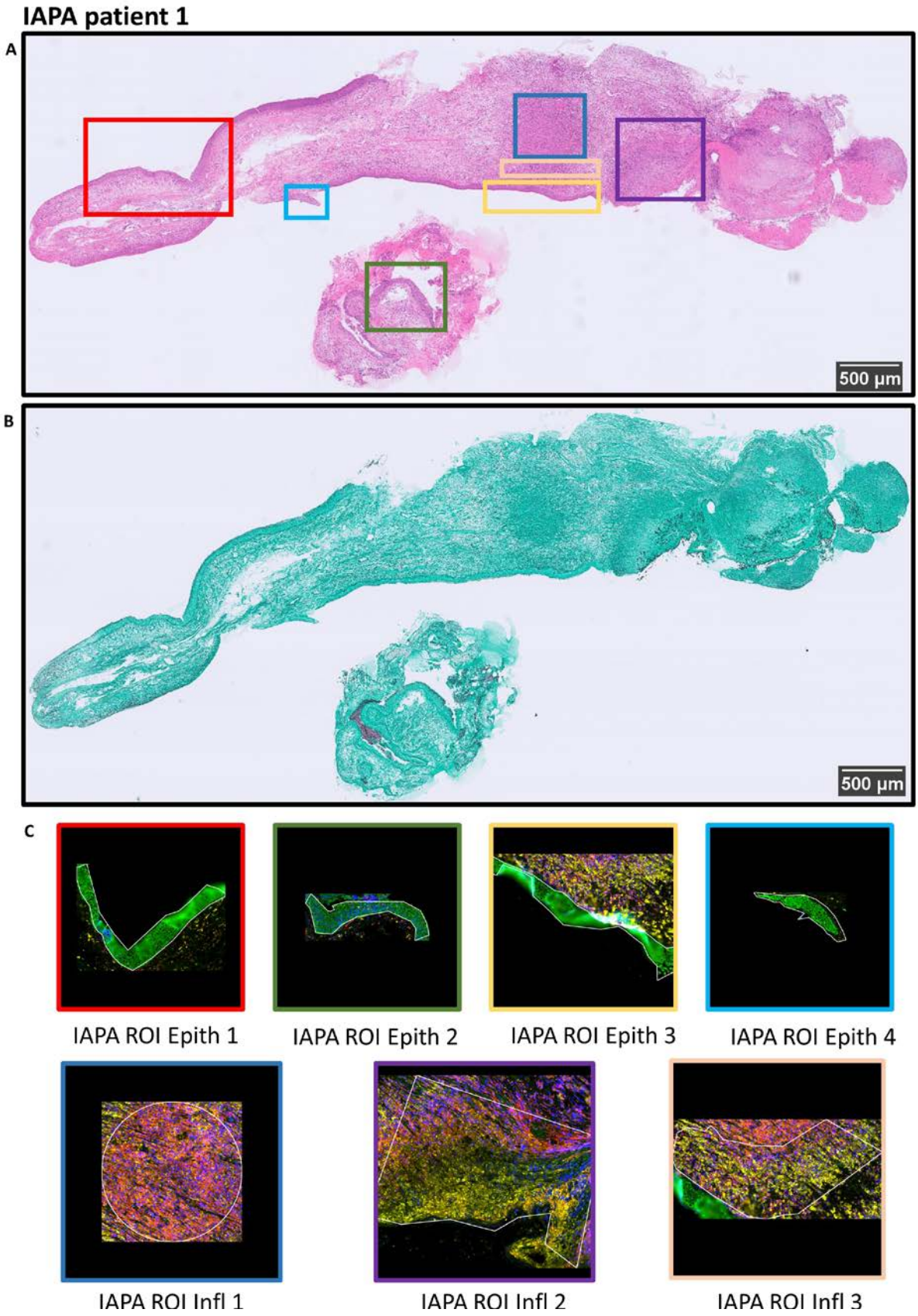

Supplementary Figure E24

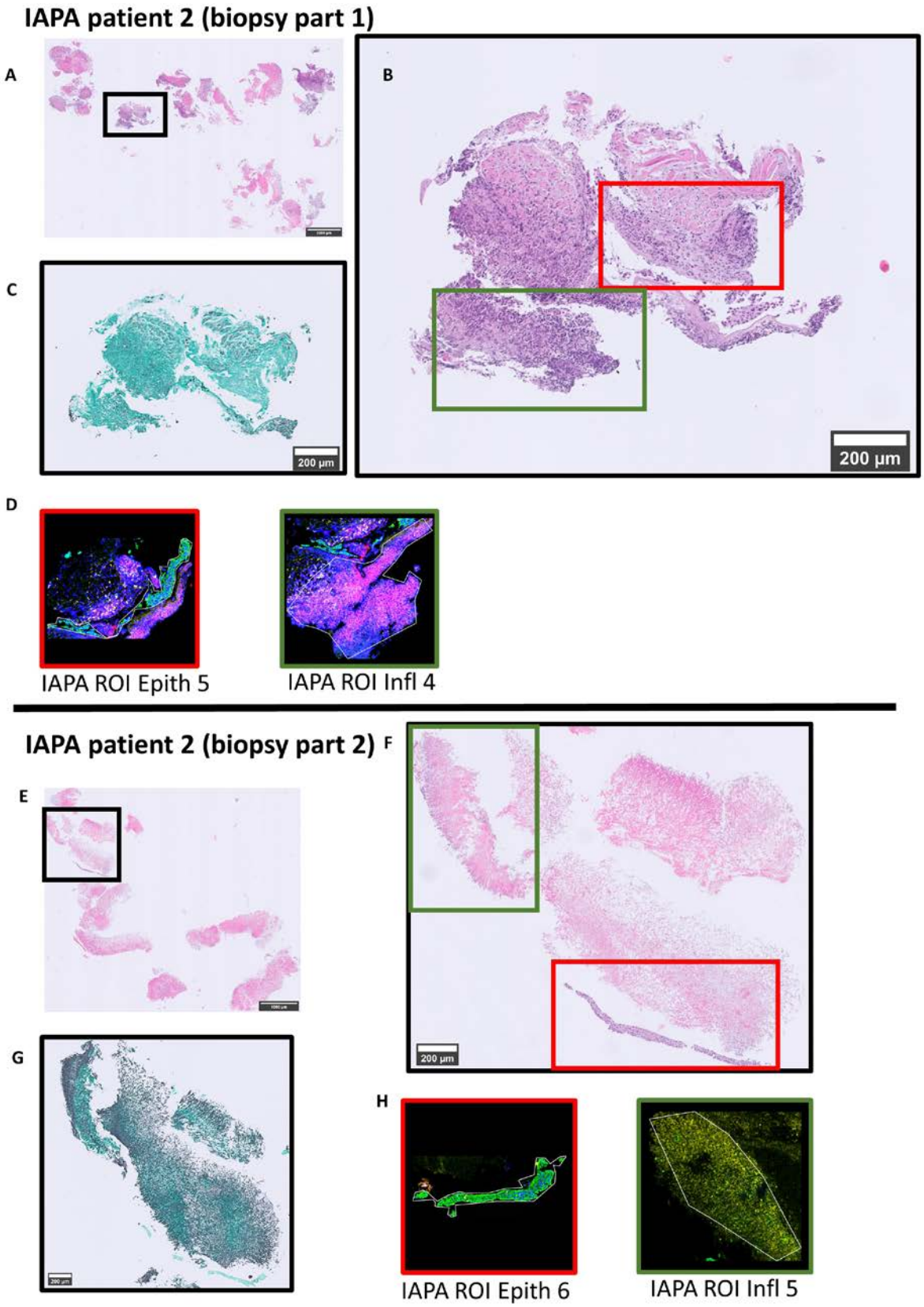

Supplementary Figure E25

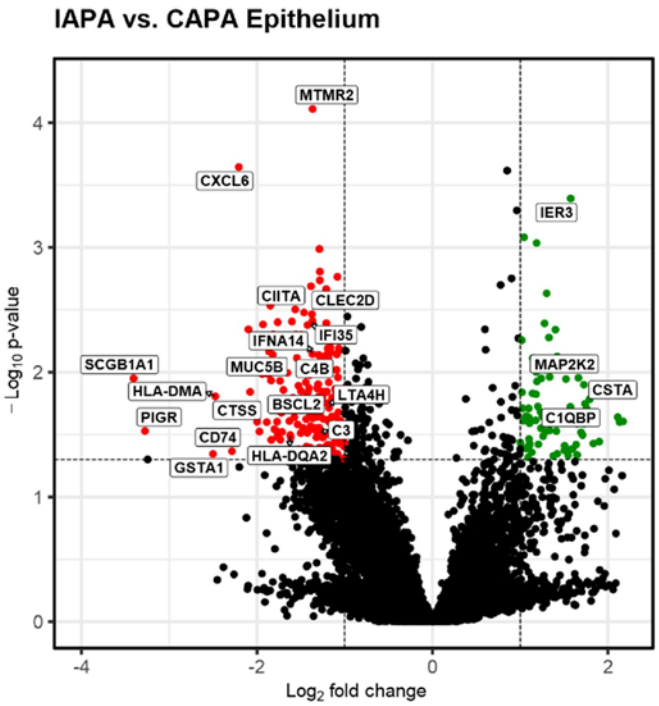

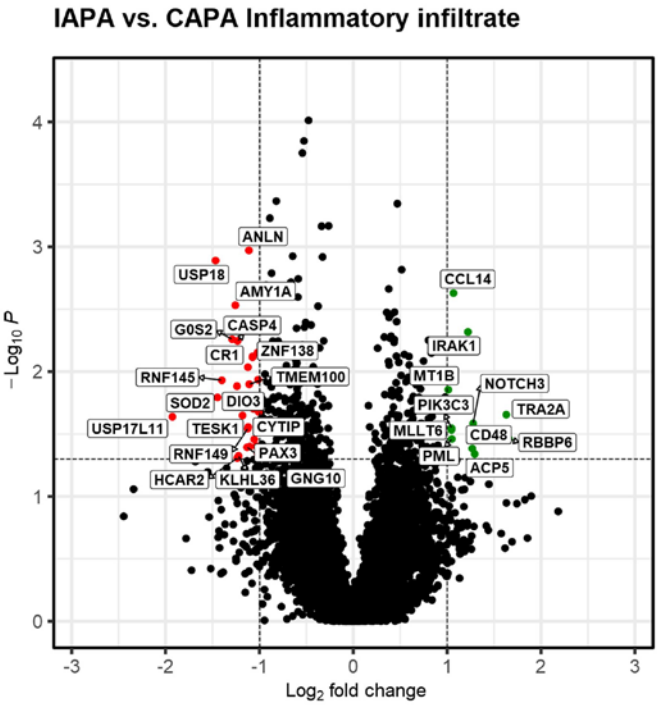

Supplementary Figure E26

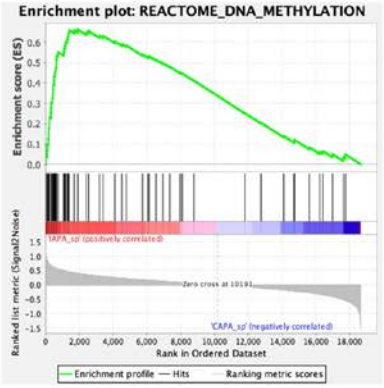

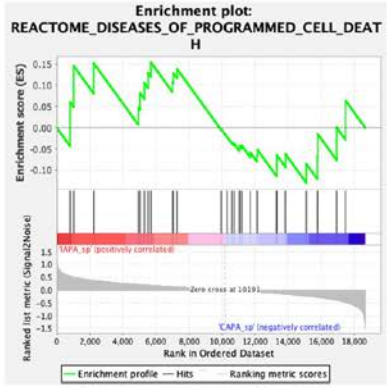

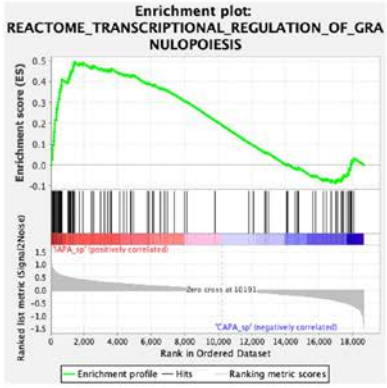

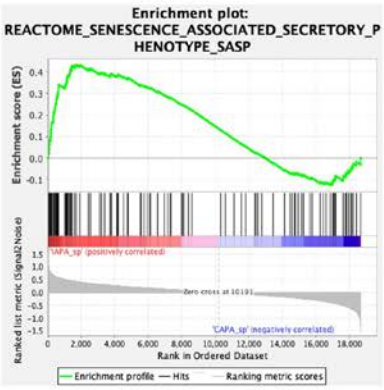

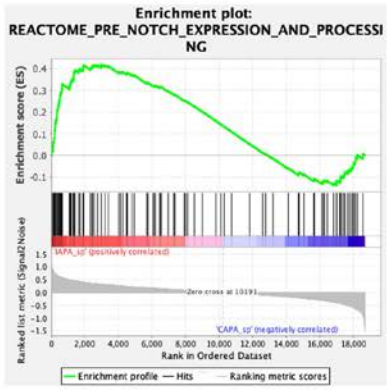

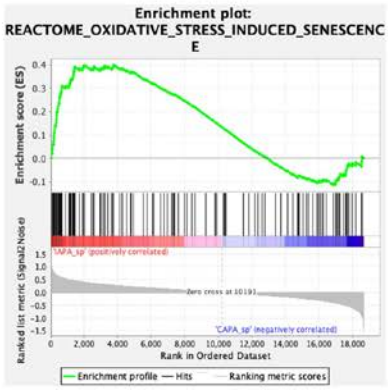

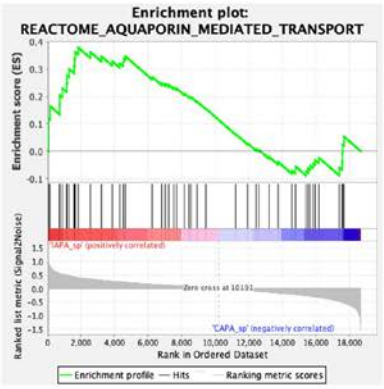

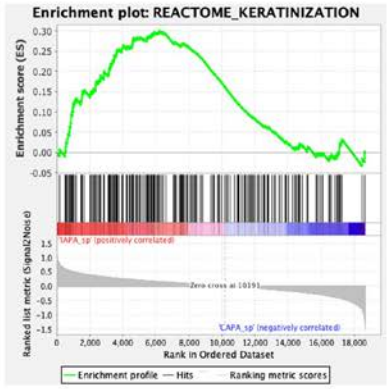

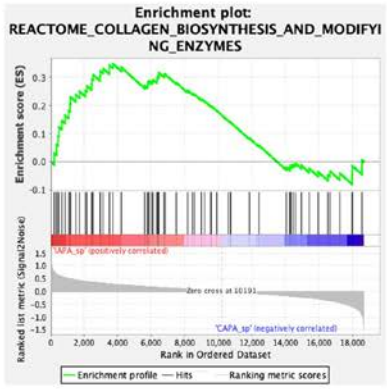

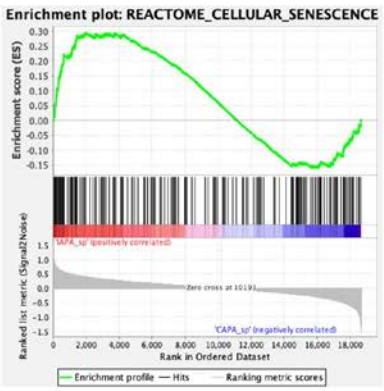

Supplementary Figure E27

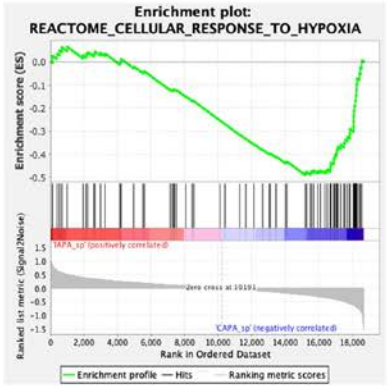

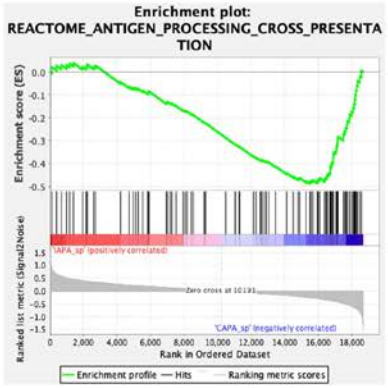

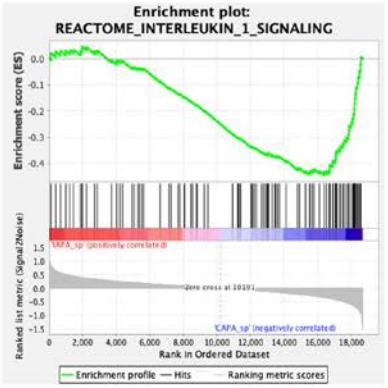

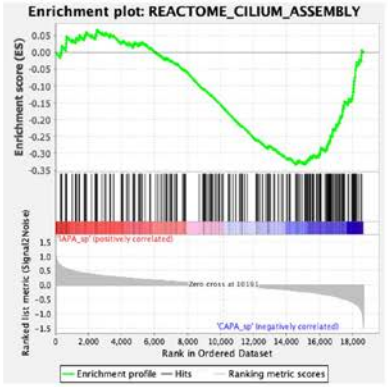

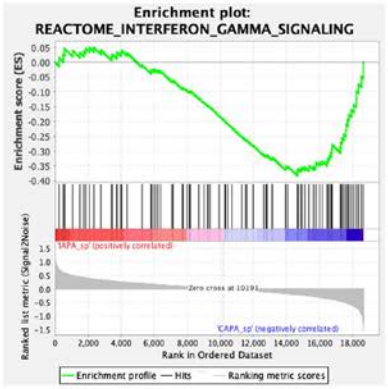

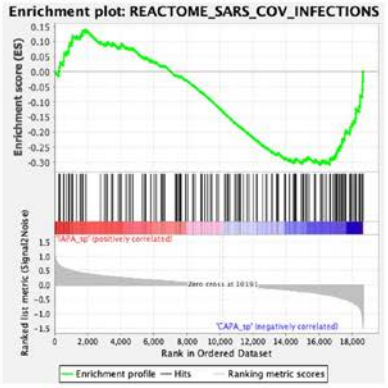

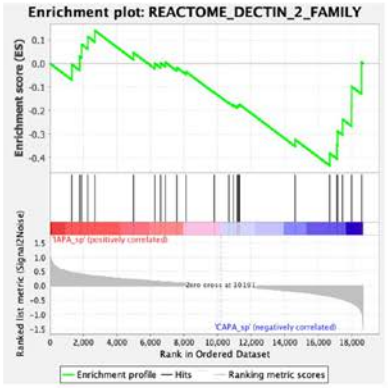

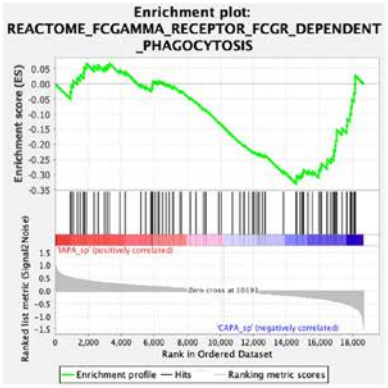

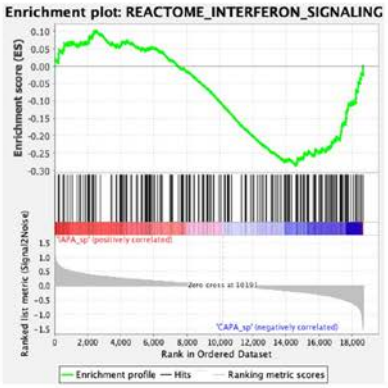

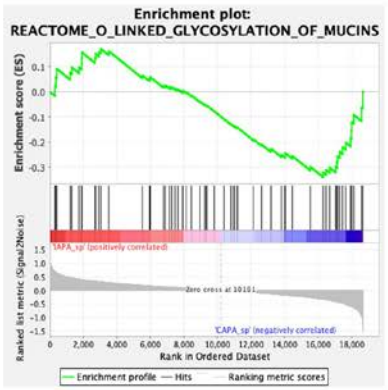

References to the Supplementary Material

1 Verweij P, Rijnders B, Brüggemann R, et al. International Expert Review of Influenza-Associated Pulmonary Aspergillosis in ICU Patients and Recommendations for a Case Definition. *Intensive Care Med* 2020; **46**: 1524–1535.

2 Koehler P, Bassetti M, Chakrabarti A, et al. Defining and managing COVID-19-associated pulmonary aspergillosis: the 2020 ECMM/ISHAM consensus criteria for research and clinical guidance. *Lancet Infect Dis* 2021; **21**: e149–62.

3 D'Haese J, Theunissen K, Vermeulen E, et al. Detection of Galactomannan in Bronchoalveolar Lavage Fluid Samples of Patients at Risk for Invasive Pulmonary Aspergillosis: Analytical and Clinical Validity. *J Clin Microbiol* 2012; **50**: 1258.

4 Moens B, Pannecouque C, López G, et al. Simultaneous RNA quantification of human and retroviral genomes reveals intact interferon signaling in HTLV-1-infected CD4+ T cell lines. *Virol J* 2012; **9**: 171.

5 Fukutani KF, Nascimento-Carvalho CM, Bouzas ML, et al. In situ Immune Signatures and Microbial Load at the Nasopharyngeal Interface in Children With Acute Respiratory Infection. *Front Microbiol* 2018; **9**: 2475.

6 Bouzas ML, Oliveira JR, Queiroz A, et al. Diagnostic accuracy of digital RNA quantification versus real-time PCR for the detection of respiratory syncytial virus in nasopharyngeal aspirates from children with acute respiratory infection. *J Clin Virol* 2018; **106**: 34–40.

7 Perkins JR, Dawes JM, McMahon SB, Bennett DLH, Orengo C, Kohl M. ReadqPCR and NormqPCR: R packages for the reading, quality checking and normalisation of RT-qPCR quantification cycle (Cq) data. *BMC Genomics* 2012; **13**: 1–8.

8 Blighe K, Rana S, Lewis M. EnhancedVolcano: Publication-ready volcano plots with enhanced colouring and labeling. Version 1.12.0. 2021. https://github.com/kevinblighe/EnhancedVolcano.

9 Hadley W. Ggplot2: Elegant Graphics for Data Analysis 2nd edn. Springer International Publishing, 2016.

10 Newman AM, Liu CL, Green MR, et al. Robust enumeration of cell subsets from tissue expression profiles. *Nat Methods* 2015; **12**: 453–7.

11 Wauters E, Van Mol P, Garg AD, et al. Discriminating mild from critical COVID-19 by innate and adaptive immune single-cell profiling of bronchoalveolar lavages. *Cell Res* 2021; **31**: 272–90.

12 Bindea G, Mlecnik B, Hackl H, et al. ClueGO: a Cytoscape plug-in to decipher functionally grouped gene ontology and pathway annotation networks. *Bioinformatics* 2009; **25**: 1091–3.

13 Subramanian A, Tamayo P, Mootha VK, et al. Gene set enrichment analysis: A knowledge-based approach for interpreting genome-wide expression profiles. *Proc Natl Acad Sci* 2005; **102**: 15545–50.

14 Liberzon A, Birger C, Thorvaldsdóttir H, Ghandi M, Mesirov JP, Tamayo P. The Molecular Signatures Database Hallmark Gene Set Collection. *Cell Syst* 2015; **1**: 417–25.

15 Bell LCK, Meydan C, Kim J, et al. Transcriptional response modules characterize IL-1β and IL-6 activity in COVID-19. *iScience* 2021; **24**: 101896.

16 Waddell SJ, Popper SJ, Rubins KH, et al. Dissecting Interferon-Induced Transcriptional Programs in Human Peripheral Blood Cells. *PLoS One* 2010; **5**: e9753.

17 Merritt CR, Ong GT, Church SE, et al. Multiplex digital spatial profiling of proteins and RNA in fixed tissue. *Nat Biotechnol* 2020; **38**: 586–99.

18 Kassambara A. 'ggpubr': 'ggplot2' Based Publication Ready Plots. Version 0.2.5. 2020. https://github.com/kassambara/ggpubr.

19 Wei T, Simko V. R package ‘corrplot’: Visualization of a Correlation Matrix. Version 0.92. 2021. https://github.com/taiyun/corrplot.

20 Donnelly JP, Chen SC, Kauffman CA, et al. Revision and Update of the Consensus Definitions of Invasive Fungal Disease From the European Organization for Research and Treatment of Cancer and the Mycoses Study Group Education and Research Consortium. *Clin Infect Dis 2020*; **71**: 1367–76.

21 Bruno M, Horst R, Pekmezovic M, et al. Data of common and species-specific transcriptional host responses to pathogenic fungi. *Data Br 2021*; **35**: 106928.